

LOCKING-FREE FINITE ELEMENT METHODS FOR POROELASTICITY*

RICARDO OYARZÚA[†] AND RICARDO RUIZ-BAIER[‡]

Abstract. We propose a new formulation along with a family of finite element schemes for the approximation of the interaction between fluid motion and linear mechanical response of a porous medium, known as Biot's consolidation problem. The steady-state version of the system is recast in terms of displacement, pressure, and volumetric stress, and both continuous and discrete formulations are analyzed as compact perturbations of invertible problems employing a Fredholm argument. In particular, the error estimates are derived independently of the Lamé constants. Numerical results indicate the satisfactory performance and competitive accuracy of the introduced methods.

Key words. poroelasticity, finite element approximation, volumetric stress formulation, compact perturbation, Fredholm alternative, error estimates stationary flow in deformable porous media

AMS subject classifications. 65N30, 76S05, 74F10, 65N15

DOI. 10.1137/15M1050082

1. Introduction. Linear poroelasticity equations consist of a momentum conservation for a porous skeleton, coupled with mass conservation of a diffusive flow within the medium. In its basic form introduced in [7], the system allows one to describe physical loading of porous layers and the change of hydraulic equilibrium in a fluid-structure system. It also serves as the classical model for the subsurface consolidation processes and it has applications in many scenarios of high practical importance, such as petroleum production, geological CO₂ sequestration, waste disposal, pile foundations, perfusion of bones and soft living tissues, etc. The success in accurately replicating poroelasticity solutions using numerical methods is often affected by the presence of two main unphysical scenarios: spurious pressure modes and volumetric locking. Here we propose a three-field formulation of the model problem, where classical finite element methods can be employed straightforwardly without the risk of producing the aforementioned phenomena. We remark that the additional third unknown introduced in the model (and containing information about stresses) is a scalar field, thus making the proposed formulation very appealing from the computational viewpoint.

Related work and specifics of this contribution. The stability of a semidiscrete finite element (FE) method applied to linear poroelasticity was studied in the early work [26]. Mixed-primal FE formulations to approximate the solid displacement, the fluid flux, and the pore pressure were introduced in [27, 28, 36]. Primal and primal-mixed discontinuous Galerkin (DG) approximations of linear poroelasticity were proposed and analyzed in [10, 24], least-squares mixed FE methods were also

*Received by the editors November 30, 2015; accepted for publication (in revised form) July 13, 2016; published electronically September 29, 2016.

<http://www.siam.org/journals/sinum/54-5/M105008.html>

Funding: This work was partially supported by CONICYT-Chile through project Anillo ACT1118 (ANANUM), by project Fondecyt 1161325, by Universidad del Bío-Bío through DIUBB project 151408 GI/VC, and by the Elsevier Mathematical Sciences Sponsorship Fund (MSSF 2016).

[†]GIMNAP, Departamento de Matemática, Universidad del Bío-Bío, Casilla 5-C, Concepción, Chile, and Centro de Investigación en Ingeniería Matemática (CII²MA), Universidad de Concepción, Concepción, Chile (royarzua@ubiobio.cl).

[‡]Corresponding author. Mathematical Institute, Oxford University, Andrew Wiles Building, Oxford OX2 6GG, UK (ruizbaier@maths.ox.ac.uk).

applied for Biot's consolidation system in [22], pressure-stabilized methods have been employed in [37, 6], and [38] presents a mixed-mixed formulation for the same problem, where the unknowns are the Cauchy stress, the displacement, the pressure and the fluid flux, and a mixed-mixed FE method follows the same continuous setting.

Our goal is to present a stable and convergent conforming FE method for the discretization of the model problem, where the volumetric contributions to the total stress are merged into an additional unknown, yielding a saddle point formulation that can be analyzed by means of a Fredholm alternative, after regarding the problem as a compact perturbation of a Stokes-like invertible system. More precisely, in the coupled variational formulation there is a zero order term with a "wrong sign" which causes the loss of invertibility of the associated operator. However, the compactness of the embedding $H^1(\Omega) \hookrightarrow L^2(\Omega)$ allows one to make use of a Fredholm alternative to analyze its solvability (see similar approaches in [11, 17, 18]). In addition, a generic Galerkin scheme is constructed, whose solvability properties follow closely those from the continuous variational form, and more importantly, given that specific FE spaces are chosen adequately, it is stable even in the incompressible limit ($\lambda \rightarrow \infty$). We emphasize that the latter means that all constants in the estimates below are independent of the Lamé parameter λ .

Outline. The layout of this paper is as follows. In the remainder of this section we recall some needed notation and general definitions. Section 2 summarizes the model equations of linear poroelasticity, including its strong and weak forms, and boundary conditions considered in the subsequent analysis. The Galerkin scheme is introduced in section 3, where the corresponding stability analysis and convergence also are derived. In particular, in section 3.3 we make precise the definition of the involved discrete spaces, recall some approximation properties, and state the theoretical error bounds. Finally, section 4 collects several numerical results and benchmark test cases illustrating the accuracy of the proposed methods.

Preliminaries. Standard notation will be adopted for Lebesgue and Sobolev spaces. Moreover, \mathbf{M} and \mathbb{M} will denote the corresponding vectorial and tensorial counterparts of the generic scalar functional space M and $\|\cdot\|$, with no subscripts, will stand for the natural norm of either an element or an operator in any product functional space. For instance, if $\Theta \subseteq \mathbf{R}^d$, $d = 2, 3$, is a domain, $\Lambda \subseteq \mathbf{R}^d$ is a Lipschitz surface, and $r > 0$, we define $\mathbf{H}^r(\Theta) := [H^r(\Theta)]^d$ and $\mathbf{H}^r(\Lambda) := [H^r(\Lambda)]^d$. By $\mathbf{0}$ we will refer to the generic null vector (including the null functional and operator), and we will denote by C and c , with or without subscripts, bars, tildes, or hats, generic constants independent of the discretization parameters, which may take different values at different occurrences.

2. Governing equations and well-posedness analysis.

2.1. Proposed three-field formulation and boundary conditions. Let us consider a homogeneous porous matrix containing a mixture of incompressible grains and interstitial fluid. We assume that this material body occupies a bounded and simply connected domain $\Omega \subset \mathbf{R}^d$, $d = 2, 3$. For all $t > 0$, given a body force $\mathbf{f}(t) : \Omega \rightarrow \mathbf{R}^d$ and a volumetric fluid source (or sink) $s(t) : \Omega \rightarrow \mathbf{R}$, the classical Biot consolidation problem (cf. [7]) consists of finding the displacements of the porous skeleton, $\mathbf{u}(t) : \Omega \rightarrow \mathbf{R}^d$ and the pore pressure of the fluid, $p(t) : \Omega \rightarrow \mathbf{R}$, such that

$$(2.1) \quad \partial_t(c_0 p + \alpha(\operatorname{div} \mathbf{u})) - \frac{1}{\eta} \operatorname{div}[\kappa(\nabla p - \rho \mathbf{g})] = s \quad \text{in } \Omega,$$

$$(2.2) \quad \boldsymbol{\sigma} = \lambda(\operatorname{div} \mathbf{u})\mathbf{I} + 2\mu\varepsilon(\mathbf{u}) - p\mathbf{I} \quad \text{in } \Omega,$$

(2.3)

$$-\operatorname{div} \boldsymbol{\sigma} = \mathbf{f} \quad \text{in } \Omega,$$

where $\boldsymbol{\sigma}$ is the total Cauchy solid stress, $\boldsymbol{\varepsilon}(\mathbf{u}) = \frac{1}{2}(\nabla \mathbf{u} + \nabla \mathbf{u}^T)$ is the infinitesimal strain tensor (symmetrized gradient of displacements), κ is the permeability of the porous solid (here assumed isotropic and satisfying $0 < \kappa_1 \leq \kappa(\mathbf{x}) \leq \kappa_2 < \infty$ for all $\mathbf{x} \in \Omega$), λ, μ are the Lamé constants of the solid, $c_0 > 0$ is the constrained specific storage coefficient, $\alpha > 0$ is the so-called Biot–Willis parameter, \mathbf{g} is the gravity acceleration (constant and aligned with the vertical direction), $\eta > 0, \rho > 0$ are the viscosity and density of the pore fluid, and the term $c_0 p + \alpha(\operatorname{div} \mathbf{u})$ represents the total fluid content in the domain (fluid pressure plus the material volume).

Notice that (2.2) states the constitutive law of the solid (differing from the classical linear elastic model in that here p is the fluid pressure), (2.3) represents momentum conservation of the porous medium (under the assumption that the solid deformations are much slower than the fluid flow rate), whereas mass conservation of the fluid obeying a Darcy regime is accounted for by (2.1). Using Hölder continuity assumptions for rather standard boundary and initial data, the solvability of (2.1)–(2.3) has been established in [30].

In order to illustrate the main ideas of the new formulation and its discretization, we will restrict the discussion to a static problem consisting of (2.2) and (2.3) coupled with the relation

$$(2.4) \quad c_0 p + \alpha(\operatorname{div} \mathbf{u}) - \frac{1}{\eta} \operatorname{div}[\kappa(\nabla p - \rho \mathbf{g})] = s \quad \text{in } \Omega,$$

arising from, e.g., Euler time discretization of (2.1) (and making abuse of notation in s). Time dependence of field variables and data can be, therefore, dropped. Let us further consider the auxiliary unknown representing the volumetric part of the total stress (also may be regarded as a pseudo total pressure) defined as

$$(2.5) \quad \phi := p - \lambda \operatorname{div} \mathbf{u}.$$

Therefore, (2.2) and (2.4) read, respectively,

$$(2.6) \quad \boldsymbol{\sigma} = 2\mu \boldsymbol{\varepsilon}(\mathbf{u}) - \phi \mathbf{I}, \quad \left(c_0 + \frac{\alpha}{\lambda} \right) p - \frac{\alpha}{\lambda} \phi - \frac{1}{\eta} \operatorname{div}[\kappa(\nabla p - \rho \mathbf{g})] = s \quad \text{in } \Omega.$$

We assume that the domain boundary is disjointly split into a part where fluid pressure is specified and a part where displacements are imposed $\partial\Omega = \bar{\Gamma}_p \cup \bar{\Gamma}_{\mathbf{u}}, \Gamma_p \cap \Gamma_{\mathbf{u}} = \emptyset$. System (2.5)–(2.6) is then complemented with suitable boundary conditions

$$(2.7) \quad p = p_{\Gamma}, \quad \boldsymbol{\sigma} \mathbf{n} = \mathbf{h} \text{ on } \Gamma_p, \quad \text{and} \quad \mathbf{u} = \mathbf{u}_{\Gamma}, \quad (\kappa \nabla p) \cdot \mathbf{n} = j \text{ on } \Gamma_{\mathbf{u}},$$

where \mathbf{n} is the exterior unit normal vector on $\partial\Omega$, \mathbf{h} is a known load vector, and j is an imposed pressure flux.

2.2. Weak formulation. Homogeneous boundary data will be assumed for the sake of conciseness of the presentation, but we stress that (2.7) can be incorporated later on, using classical lifting arguments. Let us multiply (2.3), (2.5), and (2.6) by adequate test functions and proceed to integrate by parts in such a way that second order derivatives are removed, and the following weak formulation holds: Find $\mathbf{u} \in \mathbf{H}, p \in Q, \phi \in Z$ such that

$$(2.8) \quad a_1(\mathbf{u}, \mathbf{v}) + b_1(\mathbf{v}, \phi) = F(\mathbf{v}) \quad \forall \mathbf{v} \in \mathbf{H},$$

$$(2.9) \quad a_2(p, q) - b_2(q, \phi) = G(q) \quad \forall q \in Q,$$

$$(2.10) \quad b_1(\mathbf{v}, \psi) + b_2(p, \psi) - c(\phi, \psi) = 0 \quad \forall \psi \in Z,$$

where the boundary treatment suggests defining the involved functional spaces as

$$\mathbf{H} := \mathbf{H}_{\Gamma_u}^1(\Omega) = \{\mathbf{v} \in \mathbf{H}^1(\Omega) : \mathbf{v}|_{\Gamma_u} = \mathbf{0}\}, \quad Z := L^2(\Omega),$$

$$Q := H_{\Gamma_p}^1(\Omega) = \{q \in H^1(\Omega) : q|_{\Gamma_p} = 0\},$$

and the bilinear forms $a_1 : \mathbf{H} \times \mathbf{H} \rightarrow \mathbb{R}$, $a_2 : Q \times Q \rightarrow \mathbb{R}$, $b_1 : \mathbf{H} \times Z \rightarrow \mathbb{R}$, $b_2 : Q \times Z \rightarrow \mathbb{R}$, $c : Z \times Z \rightarrow \mathbb{R}$, and linear functionals $F : \mathbf{H} \rightarrow \mathbb{R}$, $G : Q \rightarrow \mathbb{R}$ are specified in the following way:

(2.11)

$$a_1(\mathbf{u}, \mathbf{v}) := 2\mu \int_{\Omega} \boldsymbol{\varepsilon}(\mathbf{u}) : \boldsymbol{\varepsilon}(\mathbf{v}), \quad a_2(p, q) := \left(\frac{c_0}{\alpha} + \frac{1}{\lambda} \right) \int_{\Omega} pq + \frac{1}{\alpha\eta} \int_{\Omega} \kappa \nabla p \cdot \nabla q,$$

(2.12)

$$b_1(\mathbf{v}, \psi) := - \int_{\Omega} \psi \operatorname{div} \mathbf{v}, \quad b_2(q, \psi) := \frac{1}{\lambda} \int_{\Omega} q\psi, \quad c(\phi, \psi) := \frac{1}{\lambda} \int_{\Omega} \phi\psi,$$

(2.13)

$$F(\mathbf{v}) := \int_{\Omega} \mathbf{f} \cdot \mathbf{v}, \quad G(q) := \frac{\rho}{\alpha\eta} \int_{\Omega} \kappa \mathbf{g} \cdot \nabla q - \frac{\rho}{\alpha\eta} \langle \kappa \mathbf{g} \cdot \mathbf{n}, q \rangle_{\Gamma_u} + \frac{1}{\alpha} \int_{\Omega} sq,$$

where $\langle \cdot, \cdot \rangle_{\Gamma_u}$ stands for the duality pairing between $H_{00}^{-1/2}(\Gamma_u)$ and $H_{00}^{1/2}(\Gamma_u)$ and

$$H_{00}^{1/2}(\Gamma_u) := \{q|_{\Gamma_u} : q \in H^1(\Omega), \quad q = 0 \quad \text{on} \quad \Gamma_p\}.$$

In addition, we also define an auxiliary uncoupled displacement-volumetric stress problem as follows: find $(\mathbf{u}, \phi) \in \mathbf{H} \times Z$ such that

$$(2.14) \quad \mathcal{M}^{\pm}((\mathbf{u}, \phi), (\mathbf{v}, \psi)) = \mathcal{H}(\mathbf{v}, \psi) \quad \forall (\mathbf{v}, \psi) \in \mathbf{H} \times Z,$$

where

$$\mathcal{M}^{\pm}((\mathbf{u}, \phi), (\mathbf{v}, \psi)) := a_1(\mathbf{u}, \mathbf{v}) + b_1(\mathbf{v}, \phi) \pm b_1(\mathbf{u}, \psi) \quad \text{and} \quad \mathcal{H}(\mathbf{v}, \psi) = F(\mathbf{v})$$

for all $(\mathbf{u}, \phi), (\mathbf{v}, \psi) \in \mathbf{H} \times Z$.

2.3. Stability. Let us now discuss the stability properties of the bilinear forms and functionals appearing in (2.8)–(2.10). We start by observing that all the bilinear forms are bounded:

$$(2.15) \quad \begin{aligned} |a_1(\mathbf{u}, \mathbf{v})| &\leq 2\mu C_{k,2} \|\mathbf{u}\|_{1,\Omega} \|\mathbf{v}\|_{1,\Omega}, \quad \mathbf{u}, \mathbf{v} \in \mathbf{H}, \\ |a_2(p, q)| &\leq \max \left\{ \frac{c_0}{\alpha} + \frac{1}{\lambda}, \frac{\kappa_2}{\alpha\eta} \right\} \|p\|_{1,\Omega} \|q\|_{1,\Omega}, \quad p, q \in Q, \\ |b_1(\mathbf{v}, \psi)| &\leq \sqrt{d} \|\mathbf{v}\|_{1,\Omega} \|\psi\|_{0,\Omega}, \quad \mathbf{v} \in \mathbf{H}, \psi \in Z, \\ |b_2(q, \psi)| &\leq \lambda^{-1} \|q\|_{1,\Omega} \|\psi\|_{0,\Omega}, \quad q \in Q, \psi \in Z, \\ |c(\phi, \psi)| &\leq \lambda^{-1} \|\phi\|_{0,\Omega} \|\psi\|_{0,\Omega}, \quad \phi, \psi \in Z. \end{aligned}$$

Above, $C_{k,2}$ is one of the positive constants satisfying

$$(2.16) \quad C_{k,1} \|\mathbf{v}\|_{1,\Omega}^2 \leq \|\boldsymbol{\varepsilon}(\mathbf{v})\|_{0,\Omega}^2 \leq C_{k,2} \|\mathbf{v}\|_{1,\Omega}^2 \quad \forall \mathbf{v} \in \mathbf{H}.$$

In turn, the functionals F and G are also bounded:

$$(2.17) \quad |F(\mathbf{v})| \leq \|\mathbf{f}\|_{0,\Omega} \|\mathbf{v}\|_{1,\Omega}, \quad \mathbf{v} \in \mathbf{H},$$

$$|G(q)| \leq \alpha^{-1} (\rho\eta^{-1}\kappa_2 \|\mathbf{g}\|_{0,\Omega} + \rho\eta^{-1}\kappa_2 C_\Gamma \|\mathbf{g} \cdot \mathbf{n}\|_{-1/2,\Gamma_u} + \|s\|_{0,\Omega}) \|q\|_{1,\Omega}, \quad q \in Q,$$

where $C_\Gamma > 0$ is the continuity constant of the trace operator.

We now review the positivity of the forms a_1 , a_2 , and c . By using the inequality (2.16), the uniform lower bound of κ , and according to the definition of the forms a_1 , a_2 , and c , it readily follows that

$$(2.18) \quad \begin{aligned} a_1(\mathbf{v}, \mathbf{v}) &\geq 2\mu C_{k,1} \|\mathbf{v}\|_{1,\Omega}^2 \quad \forall \mathbf{v} \in \mathbf{H}, \\ a_2(q, q) &\geq \alpha^{-1} \min\{c_0, \kappa_1 \eta^{-1}\} \|q\|_{1,\Omega}^2 + \lambda^{-1} \|q\|_{0,\Omega}^2 \quad \forall q \in Q, \\ c(\psi, \psi) &= \lambda^{-1} \|\psi\|_{0,\Omega}^2 \quad \forall \psi \in Z. \end{aligned}$$

Alternatively, owing to the Poincaré inequality $|q|_{1,\Omega}^2 \geq \hat{c} \|q\|_{0,\Omega}^2$ for all $q \in Q$, the ellipticity of a_2 can be obtained through

$$(2.19) \quad a_2(q, q) \geq \frac{\kappa_1 C_p}{\alpha \eta} \|q\|_{1,\Omega}^2 + \lambda^{-1} \|q\|_{0,\Omega}^2 \quad \forall q \in Q,$$

with $C_p = \frac{\hat{c}}{1+\hat{c}} > 0$.

Finally, the bilinear form b_1 satisfies the continuous inf-sup condition (see, e.g., [20]):

$$(2.20) \quad \sup_{\mathbf{v} \in \mathbf{H} \setminus \mathbf{0}} \frac{b_1(\mathbf{v}, \psi)}{\|\mathbf{v}\|_{1,\Omega}} \geq \beta \|\psi\|_{0,\Omega} \quad \forall \psi \in Z,$$

with $\beta > 0$ only depending on Ω .

2.4. Solvability and continuous dependence result. Now, we establish the well-posedness of problem (2.8)–(2.10). We start with the corresponding continuous dependence result.

LEMMA 2.1. *Let $(\mathbf{u}, p, \phi) \in \mathbf{H} \times Q \times Z$ be a solution of the system (2.8)–(2.10). Then there exists $C_{stab} > 0$ independent of λ , such that*

$$\|\mathbf{u}\|_{1,\Omega} + \|p\|_{1,\Omega} + \|\phi\|_{0,\Omega} \leq C_{stab} (\|\mathbf{f}\|_{0,\Omega} + \|\mathbf{g}\|_{0,\Omega} + \|\mathbf{g} \cdot \mathbf{n}\|_{-1/2,\Gamma_u} + \|s\|_{0,\Omega}).$$

Proof. First, choosing $\mathbf{v} = \mathbf{u}$ in (2.8) and $\psi = \phi$ in (2.10), and combining both equations, we easily obtain

$$a_1(\mathbf{u}, \mathbf{u}) - b_2(p, \phi) + c(\phi, \phi) = F(\mathbf{u}),$$

which together with the positivity of a_1 and c in (2.18), and the continuity of b_2 and F in (2.15) and (2.17), respectively, implies

$$(2.21) \quad 2\mu C_{k,1} \|\mathbf{u}\|_{1,\Omega}^2 - \lambda^{-1} \|p\|_{1,\Omega} \|\phi\|_{0,\Omega} + \lambda^{-1} \|\phi\|_{0,\Omega}^2 \leq \|\mathbf{f}\|_{0,\Omega} \|\mathbf{u}\|_{1,\Omega}.$$

In turn, choosing $q = p$ in (2.9), we have

$$a_2(p, p) - b_2(p, \phi) = G(p),$$

which in combination with the positivity of a_2 in (2.19) and the continuity of b_2 and G in (2.15) and (2.17), respectively, implies

$$(2.22) \quad \begin{aligned} & \frac{\kappa_1 C_p}{\alpha \eta} \|p\|_{1,\Omega}^2 + \lambda^{-1} \|p\|_{0,\Omega}^2 - \lambda^{-1} \|p\|_{1,\Omega} \|\phi\|_{0,\Omega} \\ & \leq \alpha^{-1} (\rho \eta^{-1} \kappa_2 \|\mathbf{g}\|_{0,\Omega} + \rho \eta^{-1} \kappa_2 C_\Gamma \|\mathbf{g} \cdot \mathbf{n}\|_{-1/2,\Gamma_u} + \|s\|_{0,\Omega}) \|p\|_{1,\Omega}. \end{aligned}$$

Then, adding (2.21) and (2.22), and utilizing the inequality $-2ab \geq -a^2 - b^2$, we get (2.23)

$$\begin{aligned} & 2\mu C_{k,1} \|\mathbf{u}\|_{1,\Omega}^2 + \frac{\kappa_1 C_p}{\alpha \eta} \|p\|_{1,\Omega}^2 \\ & \leq \|\mathbf{f}\|_{0,\Omega} \|\mathbf{u}\|_{1,\Omega} + \alpha^{-1} (\rho \eta^{-1} \kappa_2 \|\mathbf{g}\|_{0,\Omega} + \rho \eta^{-1} \kappa_2 C_\Gamma \|\mathbf{g} \cdot \mathbf{n}\|_{-1/2,\Gamma_u} + \|s\|_{0,\Omega}) \|p\|_{1,\Omega}, \end{aligned}$$

which readily gives

$$(2.24) \quad \|\mathbf{u}\|_{1,\Omega} + \|p\|_{1,\Omega} \leq c (\|\mathbf{f}\|_{0,\Omega} + \|\mathbf{g}\|_{0,\Omega} + \|\mathbf{g} \cdot \mathbf{n}\|_{-1/2,\Gamma_u} + \|s\|_{0,\Omega}),$$

with $c > 0$ independent of λ .

Now, from the inf-sup condition (2.20) with $\psi = \phi$ and using (2.8), we obtain (2.25)

$$\beta \|\phi\|_{0,\Omega} \leq \sup_{\mathbf{v} \in \mathbf{H} \setminus \mathbf{0}} \frac{b_1(\mathbf{v}, \phi)}{\|\mathbf{v}\|_{1,\Omega}} = \sup_{\mathbf{v} \in \mathbf{H} \setminus \mathbf{0}} \frac{F(\mathbf{v}) - a_1(\mathbf{u}, \mathbf{v})}{\|\mathbf{v}\|_{1,\Omega}} \leq \|\mathbf{f}\|_{0,\Omega} + 2\mu C_{k,2} \|\mathbf{u}\|_{1,\Omega},$$

which combined with (2.24), implies

$$\|\phi\|_{0,\Omega} \leq \tilde{c} (\|\mathbf{f}\|_{0,\Omega} + \|\mathbf{g}\|_{0,\Omega} + \|\mathbf{g} \cdot \mathbf{n}\|_{-1/2,\Gamma_u} + \|s\|_{0,\Omega}).$$

The latter bound and inequality (2.24) imply the desired estimate, which concludes the proof. \square

Next, we address the unique solvability of (2.8)–(2.10). To that end, we first observe that due to the nonsymmetry of (2.8)–(2.10), its solvability analysis cannot be straightforwardly placed in the framework of the classical Babuška–Brezzi theory. We, therefore, redefine system (2.8)–(2.10) as the following operator problem: Find $\vec{\mathbf{u}} := (\mathbf{u}, p, \phi) \in \mathbb{V} := \mathbf{H} \times \mathbf{Q} \times \mathbf{Z}$, such that

$$(2.26) \quad (\mathcal{A} + \mathcal{K}) \vec{\mathbf{u}} = \mathcal{F},$$

where $\mathcal{A} : \mathbb{V} \rightarrow \mathbb{V}$, $\mathcal{K} : \mathbb{V} \rightarrow \mathbb{V}$, and $\mathcal{F} \in \mathbb{V}$ are defined as

$$(2.27) \quad \begin{aligned} \langle \mathcal{A}(\vec{\mathbf{u}}), \vec{\mathbf{v}} \rangle_{\mathbb{V} \times \mathbb{V}} &:= a_1(\mathbf{u}, \mathbf{v}) + b_1(\mathbf{v}, \phi) - b_1(\mathbf{u}, \psi) + c(\phi, \psi) + a_2(p, q), \\ \langle \mathcal{K}(\vec{\mathbf{u}}), \vec{\mathbf{v}} \rangle_{\mathbb{V} \times \mathbb{V}} &:= b_2(p, \psi) - b_2(q, \phi), \\ \langle \mathcal{F}, \vec{\mathbf{v}} \rangle_{\mathbb{V} \times \mathbb{V}} &:= F(\mathbf{v}) + G(q) \end{aligned}$$

for all $\vec{\mathbf{u}} = (\mathbf{u}, p, \phi), \vec{\mathbf{v}} = (\mathbf{v}, q, \psi) \in \mathbb{V}$.

In this way, similarly to [12, 17], if one proves that \mathcal{A} is invertible, \mathcal{K} is compact and $(\mathcal{A} + \mathcal{K})$ is injective, then the Fredholm alternative theory implies unique solvability of (2.26), and equivalently of (2.8)–(2.10).

We begin by proving the compactness of \mathcal{K} .

LEMMA 2.2. *The operator \mathcal{K} defined in (2.27) is compact.*

Proof. Let $\mathbb{B}_2 : Q \rightarrow Z$ be the operator induced by the bilinear form b_2 , that is, the operator defined by

$$\langle \mathbb{B}_2(q), \psi \rangle_{0,\Omega} = b_2(q, \psi) = \frac{1}{\lambda} \int_{\Omega} q\psi \quad \forall q \in Q, \forall \psi \in Z,$$

where $\langle \cdot, \cdot \rangle_{0,\Omega}$ denotes the inner product in $L^2(\Omega)$. Moreover, let $I : L^2(\Omega) \rightarrow L^2(\Omega)$ be the identity operator and let i_c be the compact embedding from $H^1(\Omega)$ into $L^2(\Omega)$. Then, it is straightforward to realize that $\mathbb{B}_2 = \lambda^{-1} I \circ i_c$, which implies that \mathbb{B}_2 is a compact operator, and so is \mathbb{B}_2^* .

Owing to the above, and noting that $\mathcal{K}(\vec{u}) = (\mathbf{0}, \mathbb{B}_2(p), -\mathbb{B}_2^*(\phi))$ for all $\vec{u} = (\mathbf{u}, p, \phi)$, we conclude the proof. \square

We continue with the invertibility of \mathcal{A} .

LEMMA 2.3. *The operator \mathcal{A} defined in (2.27) is invertible.*

Proof. Given $\mathcal{F} := (\mathcal{F}_H, \mathcal{F}_Q, \mathcal{F}_Z) \in \mathbb{V}$, we first observe that proving the invertibility of \mathcal{A} is equivalent to proving the existence of a unique $\vec{u} \in \mathbb{V}$, such that

$$(2.28) \quad \mathcal{A}(\vec{u}) = \mathcal{F},$$

which in turn is equivalent to proving the unique solvability of the two uncoupled problems: Find $(\mathbf{u}, \phi) \in \mathbf{H} \times Z$, such that

$$(2.29) \quad \begin{aligned} a_1(\mathbf{u}, \mathbf{v}) + b_1(\mathbf{v}, \phi) &= F_H(\mathbf{v}) \quad \forall \mathbf{v} \in \mathbf{H}, \\ b_1(\mathbf{u}, \psi) - c(\phi, \psi) &= F_Z(\psi) \quad \forall \psi \in Z, \end{aligned}$$

and: Find $p \in Q$, such that

$$(2.30) \quad a_2(p, q) = F_Q(q) \quad \forall q \in Q,$$

where F_H , F_Q , and F_Z are the functionals induced by \mathcal{F}_H , \mathcal{F}_Q , and \mathcal{F}_Z , respectively.

According to the stability properties of the forms a_1 , b_1 , and c discussed above, namely, continuity of a_1 , b_1 , and c , inf-sup of b_1 , ellipticity of a_1 , and positive-semidefinitivity of c , the well-posedness of (2.29) follows from a straightforward application of [19, Lemma 3.4]. In turn, owing to the ellipticity and continuity of a_2 , the unique solvability of (2.30) holds by virtue of the Lax–Milgram lemma. \square

The last step consists of proving injectivity of the full operator $(\mathcal{A} + \mathcal{K})$.

LEMMA 2.4. *The map $(\mathcal{A} + \mathcal{K})$ is one-to-one.*

Proof. It suffices to show that the unique solution to the homogeneous problem

$$(2.31) \quad a_1(\mathbf{u}, \mathbf{v}) + b_1(\mathbf{v}, \phi) = 0 \quad \forall \mathbf{v} \in \mathbf{H},$$

$$(2.32) \quad a_2(p, q) - b_2(q, \phi) = 0 \quad \forall q \in Q,$$

$$(2.33) \quad b_1(\mathbf{u}, \psi) + b_2(p, \psi) - c(\phi, \psi) = 0 \quad \forall \psi \in Z,$$

is the null vector in \mathbb{V} . To that end, we apply basically the same steps in the proof of Lemma 2.1. In fact, we let $(\mathbf{u}, p, \phi) \in \mathbb{V}$ be the solution of (2.31)–(2.33), choose $\mathbf{v} = \mathbf{u}$, and $\psi = \phi$ in (2.31) and (2.33), respectively, and combine the two equations to obtain

$$(2.34) \quad a_1(\mathbf{u}, \mathbf{u}) - b_2(p, \phi) + c(\phi, \phi) = 0.$$

Then, by choosing $q = p$ in (2.32) and adding the resulting equation to (2.34), we obtain

$$a_1(\mathbf{u}, \mathbf{u}) + a_2(p, p) - 2b_2(p, \phi) + c(\phi, \phi) = 0,$$

which, along with the positivity of a_1 , a_2 , and c in (2.18)–(2.19), the continuity of b_2 in (2.15), and the inequality $-2ab \geq -a^2 - b^2$, implies

$$2\mu C_{k,1} \|\mathbf{u}\|_{1,\Omega}^2 + \frac{\kappa_1 C_p}{\alpha\eta} \|p\|_{1,\Omega}^2 \leq 0.$$

From the previous inequality we readily infer that $\mathbf{u} = \mathbf{0}$ and $p = 0$. In turn, by applying the inf-sup condition of b_1 in (2.20) with $\psi = \phi$, and using (2.31) and the continuity of a_1 , we easily obtain

$$\beta \|\phi\|_{0,\Omega} \leq \sup_{\mathbf{v} \in \mathbf{H} \setminus \mathbf{0}} \frac{|b_1(\mathbf{v}, \phi)|}{\|\mathbf{v}\|_{1,\Omega}} = \sup_{\mathbf{v} \in \mathbf{H} \setminus \mathbf{0}} \frac{|a_1(\mathbf{u}, \mathbf{v})|}{\|\mathbf{v}\|_{1,\Omega}} \leq 2\mu C_{k,2} \|\mathbf{u}\|_{1,\Omega},$$

which implies that $\phi = 0$ and concludes the proof. \square

The combination of Lemmas 2.1, 2.2, 2.3, and 2.4 with the Fredholm alternative theory for compact operators implies the main result of this section, stated in the following theorem.

THEOREM 2.5. *Given $\mathbf{f} \in \mathbf{L}^2(\Omega)$, $\mathbf{g} \in \mathbf{L}^2(\Omega)$, and $s \in L^2(\Omega)$, there exists a unique solution $(\mathbf{u}, p, \phi) \in \mathbf{H} \times Q \times Z$ to the coupled problem (2.8)–(2.10). Moreover, there exists a positive constant C_{stab} , independent of λ , such that*

$$\|\mathbf{u}\|_{1,\Omega} + \|p\|_{1,\Omega} + \|\phi\|_{0,\Omega} \leq C_{stab} (\|\mathbf{f}\|_{0,\Omega} + \|\mathbf{g}\|_{0,\Omega} + \|\mathbf{g} \cdot \mathbf{n}\|_{-1/2,\Gamma_u} + \|s\|_{0,\Omega}).$$

3. The Galerkin method. In this section we introduce the Galerkin scheme of (2.8)–(2.10). By considering arbitrary finite dimensional subspaces we analyze its solvability and provide the corresponding Céa's estimate. We begin by introducing the generic discrete spaces

$$\mathbf{H}_h \subseteq \mathbf{H}, \quad Q_h \subseteq Q, \quad \text{and} \quad Z_h \subseteq Z,$$

where the subscript h stands for the size of a regular triangulation \mathcal{T}_h of $\bar{\Omega}$ made up of triangles K (when $d = 2$) or tetrahedra K , (when $d = 3$) of diameter h_K ; that is, $h := \max \{h_K : K \in \mathcal{T}_h\}$.

In this way, the Galerkin scheme associated to (2.8)–(2.10) reads as follows: Find $\mathbf{u}_h \in \mathbf{H}_h$, $p_h \in Q_h$, and $\phi_h \in Z_h$, such that

$$(3.1) \quad a_1(\mathbf{u}_h, \mathbf{v}_h) + b_1(\mathbf{v}_h, \phi_h) = F(\mathbf{v}_h) \quad \forall \mathbf{v}_h \in \mathbf{H}_h,$$

$$(3.2) \quad a_2(p_h, q_h) - b_2(q_h, \phi_h) = G(q_h) \quad \forall q_h \in Q_h,$$

$$(3.3) \quad b_1(\mathbf{u}_h, \psi_h) + b_2(p_h, \psi_h) - c(\phi_h, \psi_h) = 0 \quad \forall \psi_h \in Z_h,$$

where the bilinear forms a_1 , a_2 , b_1 , b_2 , c and the functionals F and G are defined in (2.11)–(2.13).

3.1. Existence and uniqueness of solution. It is clear that all the bilinear forms and functionals preserve the stability properties (2.15) and (2.17) on the corresponding discrete spaces. In addition, the bilinear forms a_1 , a_2 , and c preserve the positivity properties (2.18)–(2.19) on \mathbf{H}_h , Q_h , and Z_h , respectively. However, the inf-sup condition (2.20) is not necessarily inherited at the discrete level, reason why,

from now on we assume that there exists a positive constant $\hat{\beta}$, independent of h , such that

$$(3.4) \quad \sup_{\mathbf{v}_h \in \mathbf{H}_h \setminus \mathbf{0}} \frac{b_1(\mathbf{v}_h, \psi_h)}{\|\mathbf{v}_h\|_{1,\Omega}} \geq \hat{\beta} \|\psi_h\|_{0,\Omega} \quad \forall \psi_h \in Z_h.$$

As we will see next in section 3.3, the pair (\mathbf{H}_h, Z_h) can be chosen as a pair of stable finite element subspaces for the Stokes problem.

The following theorem establishes the well-posedness of the Galerkin scheme (3.1)–(3.3).

THEOREM 3.1. *Assume that the discrete inf-sup condition (3.4) holds. Then, given $\mathbf{f} \in \mathbf{L}^2(\Omega)$, $\mathbf{g} \in \mathbf{L}^2(\Omega)$, and $s \in L^2(\Omega)$, there exists a unique solution $(\mathbf{u}_h, p_h, \phi_h) \in \mathbf{H}_h \times Q_h \times Z_h$ to the discrete coupled problem (3.1)–(3.3). Moreover, there exists a positive constant \hat{C}_{stab} , independent of h and λ , such that*

$$(3.5) \quad \|\mathbf{u}_h\|_{1,\Omega} + \|p_h\|_{1,\Omega} + \|\phi_h\|_{0,\Omega} \leq \hat{C}_{stab} (\|\mathbf{f}\|_{0,\Omega} + \|\mathbf{g}\|_{0,\Omega} + \|\mathbf{g} \cdot \mathbf{n}\|_{-1/2,\Gamma_u} + \|s\|_{0,\Omega}).$$

Proof. Since \mathbf{H}_h , Q_h , and Z_h are finite dimensional spaces, for the solvability analysis it suffices to prove that the solution of the homogeneous problem is the trivial one. To do that, we let $\mathbf{u}_h \in \mathbf{H}_h$, $p_h \in Q_h$, and $\phi_h \in Z_h$ be the solution of (3.1)–(3.3) with $\mathbf{f} = \mathbf{0}$, $\mathbf{g} = \mathbf{0}$, and $s = 0$. Then, proceeding identically as in the proof of Lemma 2.4, that is, combining (3.1) and (3.3) with $\mathbf{v}_h = \mathbf{u}_h$ and $\psi_h = \phi_h$, respectively, adding (3.3) with $q_h = p_h$ to the resulting equation, and using the positivity of a_1 , a_2 , and c in (2.18)–(2.19), the continuity of b_2 in (2.15), and the inequality $-2ab \geq -a^2 - b^2$, we obtain

$$2\mu C_{k,1} \|\mathbf{u}_h\|_{1,\Omega}^2 + \frac{\kappa_1 C_p}{\alpha \eta} \|p_h\|_{1,\Omega}^2 \leq 0$$

from which $\mathbf{u}_h = \mathbf{0}$ and $p_h = 0$. Furthermore, from the inf-sup condition (3.4) with $\psi_h = \phi_h$, and the first equation of (3.1), we easily obtain $\phi_h = 0$.

Similarly, the continuous dependence result (3.5) can be derived following exactly the same steps of the proof of Lemma 2.1. We omit further details. \square

3.2. A priori error estimate. We now derive the corresponding Céa's estimate. This result is established next.

THEOREM 3.2. *Assume that the discrete inf-sup condition (3.4) holds. Let $(\mathbf{u}, p, \phi) \in \mathbf{H} \times Q \times Z$ and $(\mathbf{u}_h, p_h, \phi_h) \in \mathbf{H}_h \times Q_h \times Z_h$ be the unique solutions of the continuous and discrete coupled problems (2.8)–(2.10) and (3.1)–(3.3), respectively. Then, there exists $C_{Céa} > 0$, independent of h and λ , such that*

$$(3.6) \quad \|\mathbf{u} - \mathbf{u}_h\|_{1,\Omega} + \|p - p_h\|_{1,\Omega} + \|\phi - \phi_h\|_{0,\Omega} \leq C_{Céa} (\text{dist}(\mathbf{u}, \mathbf{H}_h) + \text{dist}(p, Q_h) + \text{dist}(\phi, Z_h)).$$

Proof. Let us first introduce the discrete space

$$\mathbf{K}_h := \{\mathbf{v}_h \in \mathbf{H}_h : b_1(\mathbf{v}_h, \psi_h) = -b_2(p_h, \psi_h) + c(\phi_h, \psi_h) \quad \forall \psi_h \in Z_h\},$$

which is clearly nonempty since $\mathbf{u}_h \in \mathbf{K}_h$ and since the discrete inf-sup condition (3.4) holds. In addition, it is not difficult to see that the following inequality holds (see, for instance, [16, Theorem 2.6]):

$$(3.7) \quad \text{dist}(\mathbf{u}, \mathbf{K}_h) \leq C \text{dist}(\mathbf{u}, \mathbf{H}_h).$$

Next, in order to simplify the subsequent analysis, we write $\mathbf{e}_u = \mathbf{u} - \mathbf{u}_h$, $e_p = p - p_h$, and $e_\phi = \phi - \phi_h$. As usual, for arbitrary $\hat{\mathbf{v}}_h \in \mathbf{K}_h$, $\hat{q}_h \in Q_h$, and $\hat{\psi}_h \in Z_h$, we shall decompose these errors into

$$(3.8) \quad \mathbf{e}_u = \mathbf{r}_u + \boldsymbol{\chi}_u, \quad e_p = r_p + \chi_p, \quad \text{and} \quad e_\phi = r_\phi + \chi_\phi,$$

with

$$(3.9) \quad \begin{aligned} \mathbf{r}_u &:= \mathbf{u} - \hat{\mathbf{v}}_h \in \mathbf{H}, & \boldsymbol{\chi}_u &:= \hat{\mathbf{v}}_h - \mathbf{u}_h \in \mathbf{H}_h, \\ r_p &:= p - \hat{q}_h \in Q, & \chi_p &:= \hat{q}_h - p_h \in Q_h, \\ r_\phi &:= \phi - \hat{\psi}_h \in Z, & \chi_\phi &:= \hat{\psi}_h - \phi_h \in Z_h. \end{aligned}$$

Notice that, since \mathbf{u}_h and $\hat{\mathbf{v}}_h$ belong to \mathbf{K}_h , then

$$b_1(\mathbf{u}_h, \psi_h) = -b_2(p_h, \psi_h) + c(\phi_h, \psi_h) \text{ and } b_1(\hat{\mathbf{v}}_h, \psi_h) = -b_2(p_h, \psi_h) + c(\phi_h, \psi_h) \quad \forall \psi_h \in Z_h.$$

It follows that

$$b_1(\boldsymbol{\chi}_u, \psi_h) = b_1(\hat{\mathbf{v}}_h - \mathbf{u}_h, \psi_h) = 0 \quad \forall \psi_h \in Z_h,$$

which implies that $\boldsymbol{\chi}_u \in \text{Ker}_h(b_1) := \{\mathbf{v}_h \in \mathbf{H}_h : b_1(\mathbf{v}_h, \psi_h) = 0 \quad \forall \psi_h \in Z_h\}$. Observe also that if we prove the existence of a positive constant C , independent of h and λ , such that

$$(3.10) \quad \|\boldsymbol{\chi}_u\|_{1,\Omega} + \|\chi_p\|_{1,\Omega} + \|\chi_\phi\|_{0,\Omega} \leq C(\|\mathbf{r}_u\|_{1,\Omega} + \|r_p\|_{1,\Omega} + \|r_\phi\|_{0,\Omega}),$$

then one could simply use the triangle inequality and the fact that $\hat{\mathbf{v}}_h$, \hat{q}_h , and $\hat{\psi}_h$ are arbitrary, to obtain

$$\|\mathbf{e}_u\|_{1,\Omega} + \|e_p\|_{1,\Omega} + \|e_\phi\|_{0,\Omega} \leq (1 + C)(\text{dist}(\mathbf{u}, \mathbf{K}_h) + \text{dist}(p, Q_h) + \text{dist}(\phi, Z_h)),$$

which, together with (3.7), implies (3.6). Therefore, in what follows we focus on proving (3.10). To that end, we first establish the corresponding Galerkin orthogonality property:

$$(3.11) \quad a_1(\mathbf{e}_u, \mathbf{v}_h) + b_1(\mathbf{v}_h, e_\phi) = 0 \quad \forall \mathbf{v}_h \in \mathbf{H}_h,$$

$$(3.12) \quad a_2(e_p, q_h) - b_2(q_h, e_\phi) = 0 \quad \forall q_h \in Q_h,$$

$$(3.13) \quad b_1(\mathbf{e}_u, \psi_h) + b_2(e_p, \psi_h) - c(e_\phi, \psi_h) = 0 \quad \forall \psi_h \in Z_h.$$

Then, from (3.11) with $\mathbf{v}_h = \boldsymbol{\chi}_u \in \text{Ker}_h(b_1)$, and considering the decomposition (3.8), we have

$$a_1(\boldsymbol{\chi}_u, \boldsymbol{\chi}_u) = -a_1(\mathbf{r}_u, \boldsymbol{\chi}_u) - b_1(\boldsymbol{\chi}_u, r_\phi),$$

which together with the ellipticity of a_1 (cf. (2.18)) and the continuity of a_1 and b_1 (cf. (2.15)), implies

$$(3.14) \quad \|\boldsymbol{\chi}_u\|_{1,\Omega} \leq C_1\{\|\mathbf{r}_u\|_{1,\Omega} + \|r_\phi\|_{0,\Omega}\},$$

with $C_1 > 0$, independent of h and λ . Notice that the latter inequality implies

$$(3.15) \quad \|\mathbf{e}_u\|_{1,\Omega} \leq (1 + C_1)\|\mathbf{r}_u\|_{1,\Omega} + C_1\|r_\phi\|_{0,\Omega}.$$

In turn, from the inf-sup condition (3.4), the first equation of (3.11), and the continuity of a_1 and b_1 (cf. (2.15)), we have

$$\begin{aligned} \|\chi_\phi\|_{0,\Omega} &\leq \beta^{-1} \sup_{\mathbf{v}_h \in \mathbf{H}_h \setminus \{\mathbf{0}\}} \frac{|b_1(\mathbf{v}_h, \chi_\phi)|}{\|\mathbf{v}_h\|_{1,\Omega}} = \beta^{-1} \sup_{\mathbf{v}_h \in \mathbf{H}_h \setminus \{\mathbf{0}\}} \frac{|a_1(\mathbf{e}_u, \mathbf{v}_h) + b_1(\mathbf{v}_h, \mathbf{r}_\phi)|}{\|\mathbf{v}_h\|_{1,\Omega}} \\ &\leq \beta^{-1} (2\mu C_{k,2} \|\mathbf{e}_u\|_{1,\Omega} + \sqrt{n} \|\mathbf{r}_\phi\|_{0,\Omega}), \end{aligned}$$

which, together with (3.15), implies

$$(3.16) \quad \|\chi_\phi\|_{0,\Omega} \leq C_2 (\|\mathbf{r}_u\|_{1,\Omega} + \|\mathbf{r}_\phi\|_{0,\Omega}),$$

with $C_2 > 0$, independent of h and λ . In addition, similarly as before, we observe that (3.16) and the triangle inequality imply

$$(3.17) \quad \|\mathbf{e}_\phi\|_{0,\Omega} \leq C_2 \|\mathbf{r}_u\|_{1,\Omega} + (1 + C_2) \|\mathbf{r}_\phi\|_{0,\Omega}.$$

Finally, from (3.12), the ellipticity of a_2 (cf. (2.19)), and the continuity of a_2 and b_2 , we obtain

$$\begin{aligned} \frac{\kappa_1 C_p}{\alpha \eta} \|\chi_p\|_{1,\Omega}^2 &\leq a_2(\chi_p, \chi_p) = -a_2(\mathbf{r}_p, \chi_p) + b_2(\chi_p, \mathbf{e}_\phi) \\ &\leq \frac{1}{\alpha} \max \left\{ c_0 + \frac{\alpha}{\lambda}, \frac{\kappa_2}{\eta} \right\} \|\mathbf{r}_p\|_{1,\Omega} \|\chi_p\|_{1,\Omega} + \lambda^{-1} \|\mathbf{e}_\phi\|_{0,\Omega} \|\chi_p\|_{1,\Omega}, \end{aligned}$$

which, together with (3.17), implies

$$(3.18) \quad \|\chi_p\|_{1,\Omega} \leq C_3 \left(\max \left\{ c_0 + \frac{\alpha}{\lambda}, \frac{\kappa_2}{\eta} \right\} \|\mathbf{r}_p\|_{1,\Omega} + \lambda^{-1} \|\mathbf{r}_u\|_{1,\Omega} + \lambda^{-1} \|\mathbf{r}_\phi\|_{0,\Omega} \right).$$

Therefore, summing up inequalities (3.14), (3.16), and (3.18), we get

$$\begin{aligned} \|\boldsymbol{\chi}_u\|_{1,\Omega} + \|\chi_p\|_{1,\Omega} + \|\chi_\phi\|_{0,\Omega} &\leq (C_1 + C_2 + \lambda^{-1} C_3) \|\mathbf{r}_u\|_{1,\Omega} \\ &\quad + C_3 \max \left\{ c_0 + \frac{\alpha}{\lambda}, \frac{\kappa_2}{\eta} \right\} \|\mathbf{r}_p\|_{1,\Omega} + (C_1 + C_2 + \lambda^{-1} C_3) \|\mathbf{r}_\phi\|_{0,\Omega}, \end{aligned}$$

which yields the result. \square

Remark 3.1. The coefficients $\max\{c_0 + \frac{\alpha}{\lambda}, \frac{\kappa_2}{\eta}\}$ and $(C_1 + C_2 + \lambda^{-1} C_3)$ in the previous inequality must be understood as constants independent of λ since, if λ goes to infinity (when the locking phenomenon occurs), $\lambda^{-1} C_3$ and $\lambda^{-1} \alpha$ are negligible.

3.3. Particular choice of finite elements. Now, we provide three concrete examples of finite elements subspaces to approximate the solution of (2.8)–(2.10). To do that, given an integer $k \geq 0$ and a set S of \mathbb{R}^d , in what follows we denote by $\mathbb{P}_k(S)$ the space of polynomial functions on S of degree $\leq k$.

Hood–Taylor + Lagrange. Let $k \geq 0$ be an integer. Then, the well-known Hood–Taylor element (see, e.g., [20]) consists of the pair (\mathbf{H}_h, Z_h) , where

$$\mathbf{H}_h := \left\{ \mathbf{v}_h \in [C(\bar{\Omega})]^d : \mathbf{v}_h|_K \in [\mathbb{P}_{k+2}(K)]^d \quad \forall K \in \mathcal{T}_h, \quad \mathbf{v}_h = 0 \text{ on } \Gamma_u \right\}$$

and

$$Z_h := \left\{ \psi_h \in C(\bar{\Omega}) : \psi_h|_K \in \mathbb{P}_{k+1}(K) \quad \forall K \in \mathcal{T}_h \right\}.$$

In turn, given an integer $l \geq 0$ to approximate the variable p we can simply choose the discrete space

$$(3.19) \quad Q_h := \{q_h \in C(\bar{\Omega}) : q_h|_K \in \mathbb{P}_{l+1}(K) \quad \forall K \in \mathcal{T}_h, \quad q_h = 0 \text{ on } \Gamma_p\}.$$

It is well known that the pair (\mathbf{H}_h, Z_h) satisfies the inf-sup condition (3.4) (see, for instance, [8, 9, 20]). This fact and Theorem 3.1 imply the well-posedness of problem (3.1)–(3.3).

Let us now recall the approximation properties of the subspaces specified above.

(AP) _{\mathbf{u}}) There exists $C > 0$, independent of h , such that for all $\mathbf{u} \in \mathbf{H}^{k+3}(\Omega)$, there holds

$$\inf_{\mathbf{v}_h \in \mathbf{H}_h} \|\mathbf{u} - \mathbf{v}_h\|_{1,\Omega} \leq Ch^{k+2} \|\mathbf{u}\|_{k+3,\Omega}.$$

(AP) _{p}) There exists $C > 0$, independent of h , such that for all $p \in \mathbf{H}^{l+2}(\Omega)$, there holds

$$\inf_{q_h \in Q_h} \|p - q_h\|_{1,\Omega} \leq Ch^{l+1} \|p\|_{l+2,\Omega}.$$

(AP) _{ϕ}) There exists $C > 0$, independent of h , such that for all $\phi \in \mathbf{H}^{k+2}(\Omega)$, there holds

$$\inf_{\psi_h \in Z_h} \|\phi - \psi_h\|_{0,\Omega} \leq Ch^{k+2} \|\phi\|_{k+2,\Omega}.$$

Owing to these approximation properties, we now can establish the theoretical rate of convergence of our method.

THEOREM 3.3. *Let $(\mathbf{u}, p, \phi) \in \mathbf{H} \times \mathbf{Q} \times \mathbf{Z}$ and $(\mathbf{u}_h, p_h, \phi_h) \in \mathbf{H}_h \times \mathbf{Q}_h \times \mathbf{Z}_h$ be the unique solutions of (2.8)–(2.10) and (3.1)–(3.3), respectively. Given, $k, l \geq 0$, assume that $\mathbf{u} \in \mathbf{H}^{k+3}(\Omega)$, $p \in \mathbf{H}^{l+1}(\Omega)$, and $\phi \in \mathbf{H}^{k+2}(\Omega)$. Then, there exist $C_1, C_2 > 0$, independent of h and λ , such that*

$$(3.20) \quad \|\mathbf{u} - \mathbf{u}_h\|_{1,\Omega} + \|p - p_h\|_{1,\Omega} + \|\phi - \phi_h\|_{0,\Omega} \leq C_1 h^{k+2} \{ \|\mathbf{u}\|_{k+3,\Omega} + \|\phi\|_{k+2,\Omega} \} + C_2 h^{l+1} \|p\|_{l+2,\Omega}.$$

Proof. The proof follows from the Céa estimate (3.6), and the approximation properties **(AP) _{\mathbf{u}}** , **(AP) _{p}** , and **(AP) _{ϕ}** . \square

Note that choosing $l = k + 1$ yields an overall convergence rate of $O(h^{k+2})$.

Remark 3.2. The assumption of additional regularity (needed for Hood–Taylor elements) is the standard theoretical requirement to derive the desired orders of convergence (see [8, 9, 20] or [13, sect. 4.2.5]). In practice, since the model problem can be regarded as a combination between the elasticity and Darcy problems, one may assume more regularity on the data and apply classical arguments for elliptic problems (cf. [21]) to ensure the desired regularity for the solution. This analysis is however beyond the scope of this paper.

MINI–element + Lagrange. In what follows, for the sake of conciseness of the presentation we restrict ourselves to the two-dimensional (2D) case. For each $K \in \mathcal{T}_h$, we let $\mathbb{P}_{1,b}(K)$ be the space (see, e.g., [20])

$$\mathbb{P}_{1,b}(K) := [\mathbb{P}_1(K) \oplus \text{span}\{b_K\}]^2,$$

where $b_K := \varphi_1 \varphi_2 \varphi_3$ is a \mathbb{P}_3 bubble function in K , and $\varphi_1, \varphi_2, \varphi_3$ are the barycentric coordinates of K . Then, the MINI-element (see, e.g., [20]) is the pair (\mathbf{H}_h, Z_h) , where

$$\mathbf{H}_h := \{\mathbf{v}_h \in [C(\bar{\Omega})]^2 : \mathbf{v}_h|_K \in \mathbb{P}_{1,b}(K) \quad \forall K \in \mathcal{T}_h, \quad \mathbf{v}_h = 0 \text{ on } \Gamma_{\mathbf{u}}\}$$

and

$$Z_h := \{\psi_h \in C(\bar{\Omega}) : \psi_h|_K \in \mathbb{P}_1(K) \quad \forall K \in \mathcal{T}_h\}.$$

In addition, to approximate the variable p we now choose the discrete space

$$Q_h := \{q_h \in C(\bar{\Omega}) : q_h|_K \in \mathbb{P}_1(K) \quad \forall K \in \mathcal{T}_h, \quad q_h = 0 \text{ on } \Gamma_p\}.$$

As for the Hood–Taylor element defined above, it is well known that the pair (\mathbf{H}_h, Z_h) satisfies the inf-sup condition (3.4) (see, for instance, [13, 20]). Then, owing to Theorem 3.1, the discrete problem (3.1)–(3.3) defined with the subspaces above is clearly well posed.

Let us now recall the approximation properties of these subspaces.

(AP) u_h There exists $C > 0$, independent of h , such that for all $\mathbf{u} \in \mathbf{H}^2(\Omega)$, there holds

$$\inf_{\mathbf{v}_h \in \mathbf{H}_h} \|\mathbf{u} - \mathbf{v}_h\|_{1,\Omega} \leq Ch\|\mathbf{u}\|_{2,\Omega}.$$

(AP) p_h There exists $C > 0$, independent of h , such that for all $p \in H^2(\Omega)$, there holds

$$\inf_{q_h \in Q_h} \|p - q_h\|_{1,\Omega} \leq Ch\|p\|_{2,\Omega}.$$

(AP) $^\phi_h$ There exists $C > 0$, independent of h , such that for all $\phi \in H^1(\Omega)$, there holds

$$\inf_{\psi_h \in Z_h} \|\phi - \psi_h\|_{0,\Omega} \leq Ch\|\phi\|_{1,\Omega}.$$

Owing to these approximation properties, we now can establish the theoretical rate of convergence of our method.

THEOREM 3.4. *Let $(\mathbf{u}, p, \phi) \in \mathbf{H} \times Q \times Z$ and $(\mathbf{u}_h, p_h, \phi_h) \in \mathbf{H}_h \times Q_h \times Z_h$ be the unique solutions of (2.8)–(2.10) and (3.1)–(3.3), respectively. Assume that $\mathbf{u} \in \mathbf{H}^2(\Omega)$, $p \in H^2(\Omega)$, and $\phi \in H^1(\Omega)$. Then, there exist $C > 0$, independent of h and λ , such that*

$$(3.21) \quad \|\mathbf{u} - \mathbf{u}_h\|_{1,\Omega} + \|p - p_h\|_{1,\Omega} + \|\phi - \phi_h\|_{0,\Omega} \leq Ch\{\|\mathbf{u}\|_{2,\Omega} + \|p\|_{2,\Omega} + \|\phi\|_{1,\Omega}\}.$$

Proof. The proof follows from the Céa estimate (3.6), and the approximation properties **(AP) u_h** , **(AP) p_h** , and **(AP) $^\phi_h$** .

Stabilized Lagrange + Lagrange. It is often desirable to provide approximations where the pair (\mathbf{H}_h, Z_h) would not necessarily fulfill the discrete inf-sup condition (3.4), but it would achieve a more general concept of stability (for weak coercivity, see (3.22) below). The stabilization consists of adding terms to the discrete problem to enforce such a condition (see [14]). The most appealing particular advantage is that equal-order discretizations for \mathbf{u} and ϕ are allowed. Therefore, for an integer $k \geq 1$ we will consider the spaces

$$\begin{aligned} \mathbf{H}_h &:= \{\mathbf{v}_h \in [C(\bar{\Omega})]^d : \mathbf{v}_h|_K \in [\mathbb{P}_k(K)]^d \quad \forall K \in \mathcal{T}_h, \quad \mathbf{v}_h = 0 \text{ on } \Gamma_{\mathbf{u}}\}, \\ Z_h &:= \{\psi_h \in C(\bar{\Omega}) : \psi_h|_K \in \mathbb{P}_k(K) \quad \forall K \in \mathcal{T}_h\}. \end{aligned}$$

LEMMA 3.5 (see [2]). *Assume $\mathcal{H} : \mathbf{W} \rightarrow \mathbb{R}$ is a continuous and linear functional, \mathbf{W}_h is a closed subspace of \mathbf{W} , and the bilinear form $\mathcal{M}(\cdot, \cdot)$ is either coercive or it satisfies the discrete weak coercivity conditions:*

$$(3.22) \quad \sup_{\mathbf{s}_h \in \mathbf{W}_h \setminus \mathbf{0}} \frac{\mathcal{M}(\mathbf{w}_h, \mathbf{s}_h)}{\|\mathbf{s}_h\|_{\mathbf{W}}} \geq C_1^{\mathbf{W}} \|\mathbf{w}_h\|_{\mathbf{W}} \quad \forall \mathbf{w}_h \in \mathbf{W}_h \quad \text{and}$$

$$\sup_{\mathbf{w}_h \in \mathbf{W}_h} \mathcal{M}(\mathbf{w}_h, \mathbf{s}_h) > 0 \quad \forall \mathbf{s}_h \in \mathbf{W}_h \setminus \{\mathbf{0}\}.$$

Then we have the following problem: find $\mathbf{w}_h \in \mathbf{W}_h$ such that

$$\mathcal{M}(\mathbf{w}_h, \mathbf{s}_h) = \mathcal{H}(\mathbf{s}_h) \quad \forall \mathbf{s}_h \in \mathbf{W}_h$$

has a unique solution satisfying $\|\mathbf{w}_h\|_{\mathbf{W}} \leq C_2^{\mathbf{W}} \|\mathcal{H}\|_{\mathbf{W}'}$. Moreover,

$$\|\mathbf{w} - \mathbf{w}_h\|_{\mathbf{W}} \leq \left(1 + \frac{C_1^{\mathbf{W}}}{C_2^{\mathbf{W}}}\right) \inf_{\mathbf{s}_h \in \mathbf{W}_h} \|\mathbf{w} - \mathbf{s}_h\|_{\mathbf{W}}.$$

In general, embedding the additional terms into expressions that vanish when the solution is sufficiently regular (for instance, residual contributions), leads to strong consistency of the stabilized scheme. A rich variety of stabilized methods targeted for Stokes equations is available from the literature (including e.g., pressure-projection stabilizations, variational multiscale methods, etc.) but here we focus only on one family of methods known as Reflected Galerkin Least Squares (RGLS) schemes (see, e.g., the review paper [5]). They consist of approximating the problem for displacement and volumetric stress (2.14) by the augmented discrete problem

$$(3.23) \quad \mathcal{M}_{\text{RGLS}}^-((\mathbf{u}_h, \phi_h), (\mathbf{v}_h, \psi_h)) = \mathcal{H}_{\text{RGLS}}^-(\mathbf{v}_h, \psi_h) \quad \forall (\mathbf{v}_h, \psi_h) \in \mathbf{H}_h \times \mathbf{Z}_h,$$

where

$$\begin{aligned} \mathcal{M}_{\text{RGLS}}^\pm((\mathbf{u}_h, \phi_h), (\mathbf{v}_h, \psi_h)) &:= \mathcal{M}^\pm((\mathbf{u}_h, \phi_h), (\mathbf{v}_h, \psi_h)) \\ &\quad + \tau \sum_{K \in \mathcal{T}_h} h_K^2 (-2\mu \mathbf{div}[\boldsymbol{\varepsilon}(\mathbf{u}_h)] + \nabla \phi_h, -2\mu \mathbf{div}[\boldsymbol{\varepsilon}(\mathbf{v}_h)] \mp \nabla \psi_h)_{0,K}, \\ \mathcal{H}_{\text{RGLS}}^\pm(\mathbf{v}_h, \psi_h) &:= \mathcal{H}(\mathbf{v}_h, \psi_h) + \tau \sum_{K \in \mathcal{T}_h} h_K^2 (\mathbf{f}, -2\mu \mathbf{div}[\boldsymbol{\varepsilon}(\mathbf{v}_h)] \mp \nabla \psi_h)_{0,K} \end{aligned}$$

for a given stabilization constant $\tau > 0$. It can be proved that the nonsymmetric form $\mathcal{M}_{\text{RGLS}}^-(\cdot, \cdot)$ is strongly coercive for any positive τ . Therefore, problem (3.23) is uniquely solvable and unconditionally stable in the sense of Lemma 3.5 using $\mathbf{W} = \mathbf{H} \times \mathbf{Z}$ (see also [5, sect. 3.1]). If we take \mathcal{M}^+ in the definition of scheme (3.23), then we end up with the classical Douglas–Wang scheme, and for $k = 1$, the problem (3.23) boils down to

$$\begin{aligned} (3.24) \quad a_1(\mathbf{u}_h, \mathbf{v}_h) + b_1(\phi_h, \mathbf{v}_h) - b_1(\psi_h, \mathbf{u}_h) + \tau \sum_{K \in \mathcal{T}_h} h_K^2 (\nabla \phi_h, \nabla \psi_h)_{0,K} \\ = F(\mathbf{v}_h) + \tau \sum_{K \in \mathcal{T}_h} h_K^2 (\mathbf{f}, \nabla \psi_h)_{0,K}. \end{aligned}$$

If one drops the last term in the right-hand side (RHS) of (3.24), then we recover the reflected version of the classical Brezzi–Pitkäranta method.

Convergence rates for stabilized methods depend on the stabilization parameters and on the order of the approximations k . For RGLS discretizations, the choice of τ does not affect the expected convergence rates: $O(h^{k+1})$ for displacements in the L^2 -norm and $O(h^k)$ in the H^1 -norm, whereas a decay of $O(h^k)$ is expected for the volumetric stress error in the L^2 -norm (see [14]). Looking now at the pressure approximation, we choose Q_h as in the previous two FE families. Therefore, the following convergence result holds.

THEOREM 3.6. Let $(\mathbf{u}, p, \phi) \in \mathbf{H} \times Q \times Z$ and $(\mathbf{u}_h, p_h, \phi_h) \in \mathbf{H}_h \times Q_h \times Z_h$ be the unique solutions of (2.8)–(2.10) and (3.1)–(3.3), respectively. Assume that $\mathbf{u} \in \mathbf{H}^{k+1}(\Omega)$, $p \in H^{k+1}(\Omega)$, and $\phi \in H^k(\Omega)$. Then, there exists $C > 0$, independent of h and λ , such that

$$\|\mathbf{u} - \mathbf{u}_h\|_{1,\Omega} + \|p - p_h\|_{1,\Omega} + \|\phi - \phi_h\|_{0,\Omega} \leq Ch^k \{ \|\mathbf{u}\|_{k+1,\Omega} + \|p\|_{k+1,\Omega} + \|\phi\|_{k,\Omega} \}.$$

Finally, we stress that regarding poroelasticity formulations, only a few stabilization strategies have been applied to Biot consolidation problem, including a Galerkin least squares method [33], a pressure-projection scheme [6], and pressure stabilization [1] (see also [3, 4, 35] for similar schemes tailored for coupled flow-poroelasticity, finite elasticity, and geomechanics-multiphase flow equations, respectively). We also point out that the regularity of the pressure profiles is typically rather low (cf. [27, 28]), which makes the use of stabilized *low order* methods more attractive than, e.g., Hood–Taylor elements (see also Remark 3.2).

Remark 3.3. The continuous and discrete inf-sup conditions (resp., (2.20) and (3.4)), are strictly necessary to obtain all the required estimates independent of the parameter λ . In other words, without requiring these inf-sup conditions, it is still possible to prove well-posedness of the continuous and discrete problems and the corresponding Céa estimate. In fact, after simple computations, and without using the inf-sup conditions, one can readily obtain that the operator \mathcal{A} (cf. (2.27)) is invertible and $\mathcal{A} + \mathcal{K}$ is injective. However, by doing so one unfortunately obtains the continuous dependence result and the Céa estimate with constants depending on λ which leads to unstable methods when using, for example, a $[\mathbb{P}_1]^d \times \mathbb{P}_1 \times \mathbb{P}_0$ approximation, and λ is large (see Example 1 in section 4 below).

4. Numerical tests. We now provide a set of numerical examples putting into evidence some of the features analyzed above. Namely, optimal convergence in the sense of Theorems 3.3, 3.4, and 3.6, and the locking-free property.

Example 1: Convergence rates for a manufactured solution in two dimensions. Let us consider a cantilever bracket with curved boundary, where we propose the following smooth exact solutions to (2.3), (2.5), and (2.6):

(4.1)

$$\mathbf{u} = a \begin{pmatrix} \sin(\pi x_1) \cos(\pi x_2) + \frac{x_1^2}{2\lambda} \\ -\cos(\pi x_1) \sin(\pi x_2) + \frac{x_2^2}{2\lambda} \end{pmatrix}, \quad p = b \sin(\pi x_1) \sin(\pi x_2), \quad \phi = p - \lambda \operatorname{div} \mathbf{u},$$

and where the body force \mathbf{f} and fluid source s can be simply determined from (4.1). Notice that the forcing term remains bounded even for $\lambda \rightarrow \infty$, and robustness with respect to ν would be expected.

We choose the following set of model parameters: displacement and pressure scalings $a = 1e-4$, $b = \pi$; Young modulus $E = 1e4$, material permeability $\kappa = 1e-7$, Biot–Willis coefficient $\alpha = 0.1$, constrained specific storage $c_0 = 1e-5$, and the Lamé constants are $\lambda = E\nu(1+\nu)^{-1}(1-2\nu)^{-1}$, $\mu = E/(2+2\nu)$. Here, and in all subsequent tests, we consider zero gravitational forces. Note that $\operatorname{div} \mathbf{u} = a \frac{x_1+x_2}{\lambda}$, so the model approaches the incompressibility limit as $\lambda \rightarrow \infty$.

The domain Ω is delimited by four curved boundaries parametrized as

$$\Gamma_1 = \{\omega \in [0, 1] : x_1 = \omega + \gamma \cos(\pi\omega) \sin(\pi\omega), x_2 = -\gamma \cos(\pi\omega) \sin(\pi\omega)\},$$

$$\Gamma_2 = \{\omega \in [0, 1] : x_1 = 1 + \gamma \cos(\pi\omega) \sin(\pi\omega), x_2 = \omega - \gamma \cos(\pi\omega) \sin(\pi\omega)\},$$

$$\Gamma_3 = \{\omega \in [1, 0] : x_1 = \omega + \gamma \cos(\pi\omega) \sin(\pi\omega), x_2 = 1 - \gamma \cos(\pi\omega) \sin(\pi\omega)\},$$

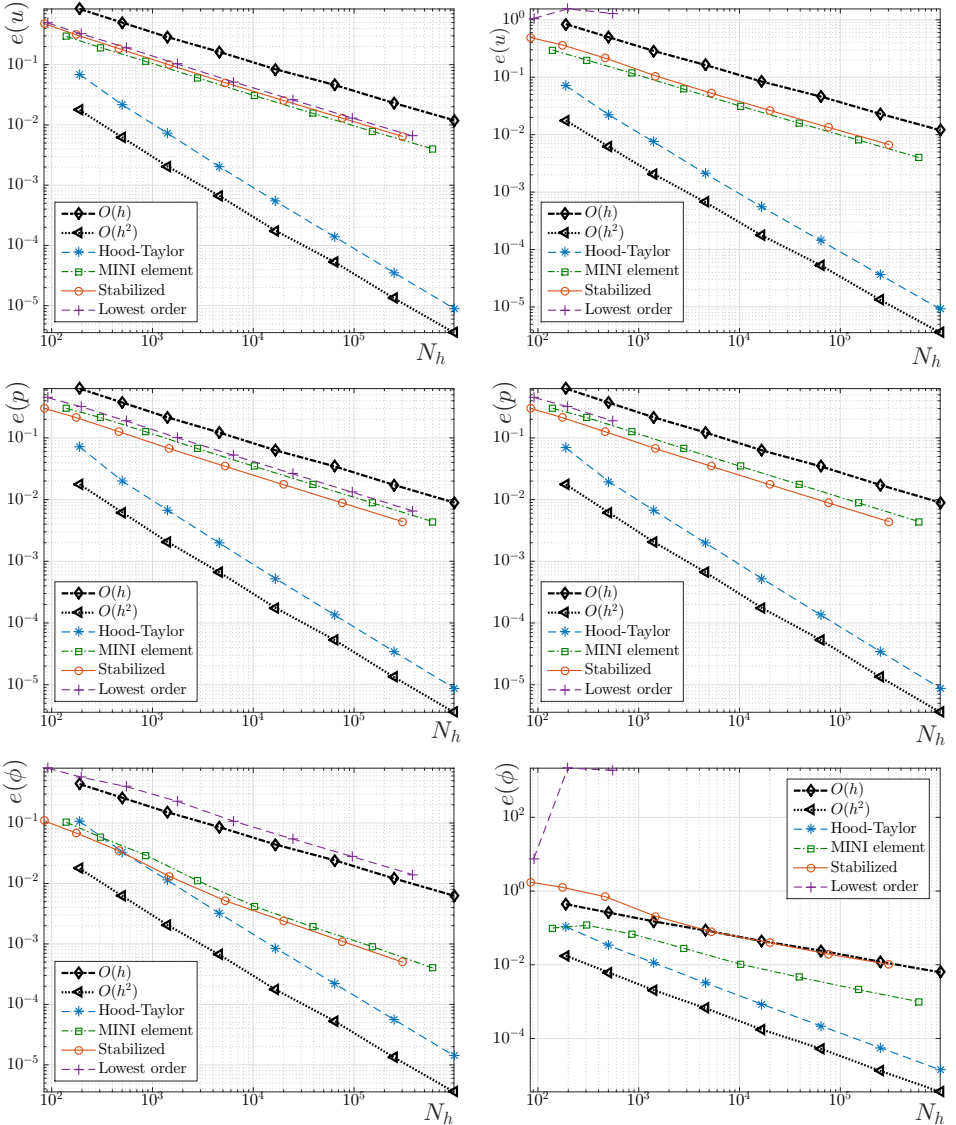


FIG. 1. Example 1: Error history associated with the exact solutions (4.1) using four different discretizations, where “Hood–Taylor” refers to the $\mathbb{P}_2^d \times \mathbb{P}_2 \times \mathbb{P}_1$ method and “lowest order” refers to the $\mathbb{P}_1^d \times \mathbb{P}_1 \times \mathbb{P}_0$ family. Panels on the left report errors incurred for $\nu = 0.4$, whereas the right plots correspond to $\nu = 0.49999$. The vertical labels indicate relative errors.

$$\Gamma_4 = \{\omega \in [1, 0] : x_1 = \gamma \cos(\pi\omega) \sin(\pi\omega), x_2 = \omega - \gamma \cos(\pi\omega) \sin(\pi\omega)\},$$

where we take $\gamma = -0.08$ (see, e.g., [29]). Boundary conditions are assigned as follows: Nonhomogeneous Dirichlet displacements and pressure normal fluxes j are set according to (4.1) on $\Gamma_u = \Gamma_3 \cup \Gamma_4$; nonhomogeneous Dirichlet pressure and Cauchy normal fluxes \mathbf{h} are set according to (4.1) on $\Gamma_p = \Gamma_1 \cup \Gamma_2$.

The accuracy of the numerical approximation using the FE families listed in section 3.3 (Hood–Taylor with $l = k + 1$, MINI-element, and stabilized scheme (3.24)) is assessed by partitioning Ω into unstructured triangulations generated putting 2^{n+1}

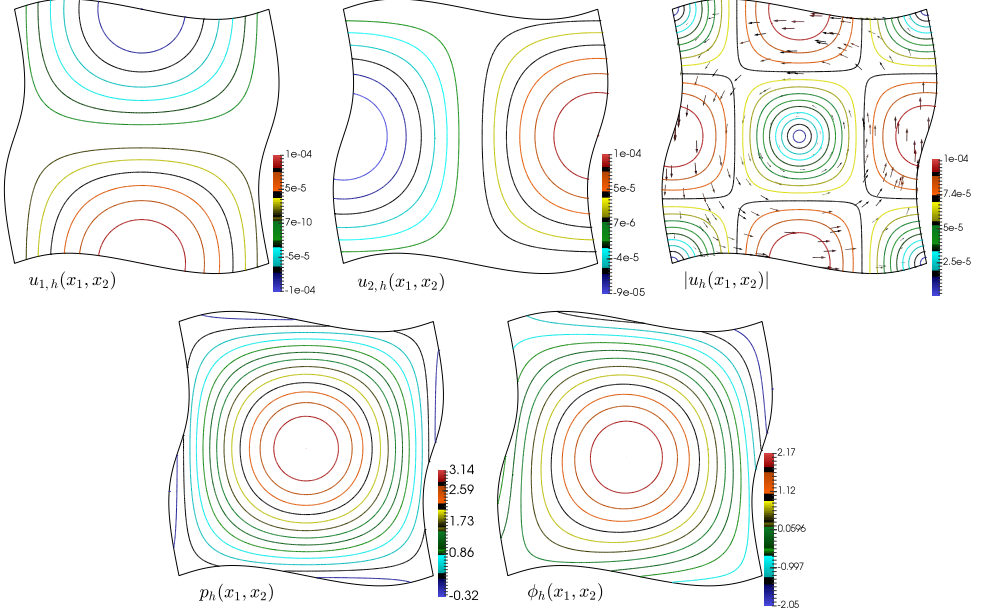


FIG. 2. Example 1: Three-field poroelasticity equations discretized with a stabilized method. This figure contains contour plots of the approximate displacement components, displacement magnitude and vectors, pressure profiles, and volumetric stress in the case where $\eta = 0.49999$ and $\lambda = 1.66e8$.

($n = 0, 1, \dots, 8$) vertices on each curve of the domain boundary. Relative errors

$$e(\mathbf{u}) := \frac{\|\mathbf{u} - \mathbf{u}_h\|_{1,\Omega}}{\|\mathbf{u}\|_{1,\Omega}}, \quad e(p) := \frac{\|p - p_h\|_{1,\Omega}}{\|p\|_{1,\Omega}}, \quad e(\phi) := \frac{\|\phi - \phi_h\|_{0,\Omega}}{\|\phi\|_{0,\Omega}},$$

between exact and approximate solutions are to be computed on each refinement level, and two sets of simulations were performed in order to study the influence of the Poisson ratio. The first case corresponds to a mild incompressibility $\nu = 0.4$ and $\lambda = 14285.7$, whereas the second case focuses on a quasi-incompressible regime with $\nu = 0.49999$ and $\lambda = 1.66e8$. Figure 1 reports on the error history. In the first case, we observe optimal convergence rates for all methods, even for a lowest order discretization using $[\mathbb{P}_1]^d \times \mathbb{P}_1 \times \mathbb{P}_0$ elements (see left panels in Figure 1). We also observe that, for the inf-sup stable methods, not only are the convergence rates invariant to increasing the Poisson ratio, but also the magnitude of the relative errors remain unchanged. The lowest-order method, on the other hand, does not even converge after three refinement steps, as evidenced in the dashed lines with a + mark on the right panels of Figure 1. In Figure 2 we illustrate the converged numerical solution obtained with the stabilized method (3.24), with stabilization constant $\tau = 1/60$. These snapshots correspond to the case $\nu = 0.49999$ and $\lambda = 1.66e8$.

Example 2: Footing problem and spurious pressure modes. We now focus on the behavior of the proposed methods when applied to the solution of the 2D *footing test*. The goal is to observe pressure, volumetric stress, and the displacements incurred after a rectangular block of porous soil undergoes a load of intensity σ_0 along a strip on top of it. The model parameters are $\Omega = (-50, 50) \times (0, 75)$, $E = 3e4 \text{ N/m}^2$, $\kappa = 1e-4 \text{ m}^2/\text{Pa}$, $\sigma_0 = 1.5e4 \text{ N/m}^2$ (see a similar test in [15] for moderate Poisson ratios). In addition, we put $c_0 = 1e-3$, $\alpha = 0.1$, and here we force the incompressibility

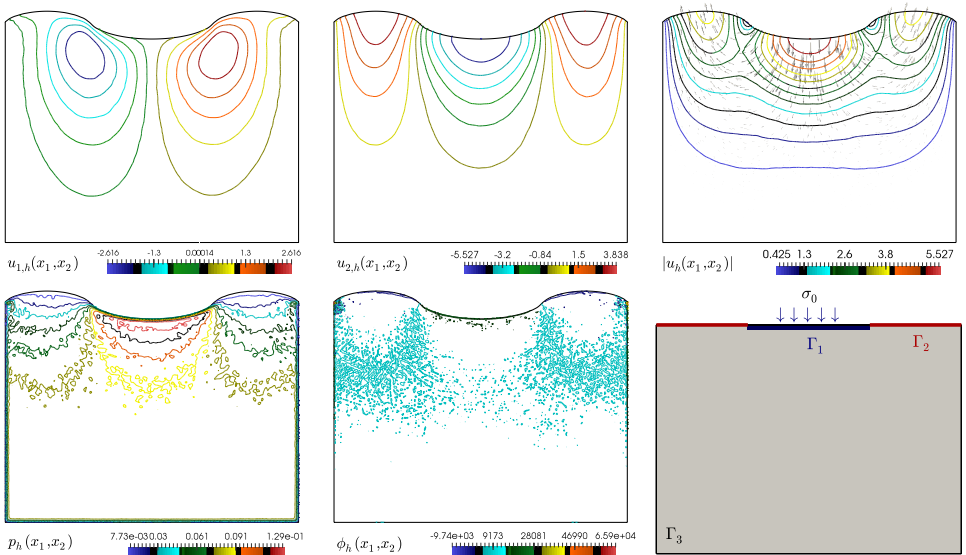


FIG. 3. Example 2: Footing of a porous block using the lowest order discretization. From top left to bottom right: Approximation of displacement components and magnitude, pressure distribution, and volumetric stress; and a sketch of the undeformed domain and boundary splitting.

limit by setting $\nu = 0.4995$. Boundary conditions are set as follows (see a sketch in the bottom right panel of Figure 3): $\mathbf{u} = \mathbf{0}$ on Γ_3 (left, right, and bottom sides of the block); $\boldsymbol{\sigma}\mathbf{n} = \mathbf{h}$ on $\Gamma_1 \cup \Gamma_2$, where $\mathbf{h} = (0, -\sigma_0)^T$ on Γ_1 and $\mathbf{h} = \mathbf{0}$ otherwise; and $p = 0$ on $\partial\Omega$. The domain is partitioned into 71272 unstructured triangles using 35637 vertices.

The value of the Poisson ratio suggests that inf-sup unstable discretizations of displacement and volumetric stress will produce spurious pressure modes. This phenomenon is evidenced in Figure 3, where we depict the numerical solution obtained with the lowest order discretization (i.e., the $[\mathbb{P}_1]^d \times \mathbb{P}_1 \times \mathbb{P}_0$ family). Both the volumetric stress and the pressure profiles are populated with oscillations, even with a quite fine mesh. On the other hand, at least in this particular case, the computed displacements do not appear to suffer from locking. Next we perform again the same test, this time using the MINI-element for the discretization of displacement and volumetric stress, whereas the pressure field is approximated with piecewise linear continuous elements. In contrast with the results collected in Figure 3, now in Figure 4 the pressure and volumetric stress fields are stable and completely free from spurious oscillations.

Example 3: Swelling of a sponge. Next, the implementation of the proposed schemes in three dimensions is tested by looking at the displacements incurred by swelling a porous block occupying the domain $\Omega = (0, 1) \times (0, 1) \times (0, \frac{1}{2})$. The driving effect is simply a pressure difference between the sides $x_1 = 0$ and $x_1 = 1$, going from $p = 1e4$ at $x_1 = 0$ to zero pressure on $x_1 = 1$. Zero-flux conditions are imposed for pressure on the remainder of the boundary. The normal components of the displacements are set to zero on the sides $x_1 = 0$, $x_2 = 0$, and $x_3 = 0$, whereas zero normal stress is considered elsewhere on $\partial\Omega$. Other model and discretization parameters are listed in what follows: $E = 8000$, $\nu = 0.3$, $c_0 = 0.001$, $\kappa = 1e-5$, $\rho = \alpha = 1$, $\tau = 1/60$. No external or internal forces are considered, neither fluid sources nor sinks.

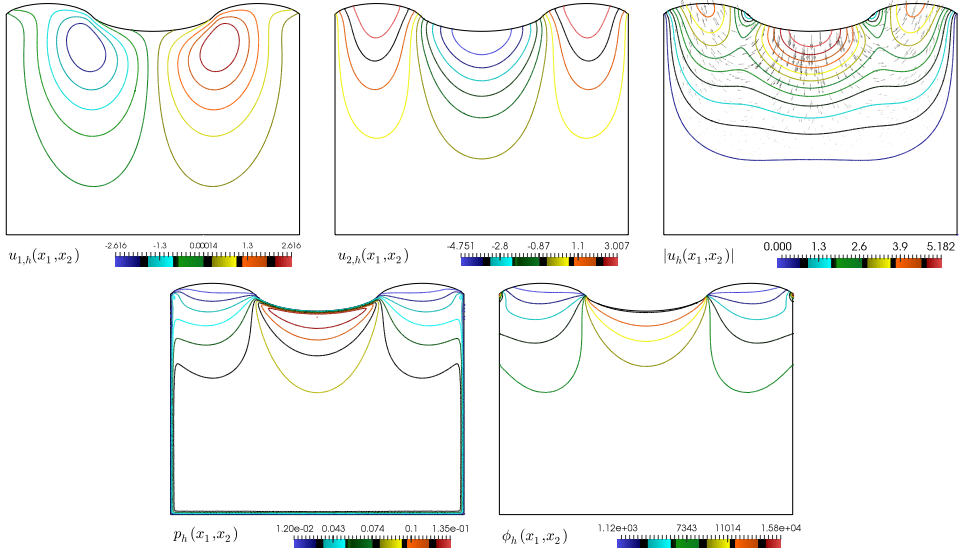


FIG. 4. Example 2: Footing of a porous block using the MINI-element method. From top left to bottom right: Approximation of displacement components and magnitude, pressure distribution, and volumetric stress.

The domain is partitioned into a structured tetrahedral mesh of 62586 elements and 10976 vertices, and a stabilized method using (3.24) is employed for the numerical approximation of displacements, volumetric stress, and pressure. The obtained results are depicted in Figure 5, where no pressure oscillations nor unphysically small displacements are observed. We also simulate the swelling of an heterogeneous porous medium, where we consider that the permeability is zero in the strip $0.45 \leq x_1 \leq 0.55$ and otherwise we take $\kappa = 1$ (that is, five orders of magnitude larger than in the previous test). Zones of zero permeability are commonly encountered in simulation of heterogeneous porous skeletons and layered media [31]. Notice that in classical formulations, the inverse of κ appears in the momentum equation, and thus the problem may degenerate (see [34]). However, system (2.8)–(2.10) is still (at least formally) solvable since a pressure mass term remains in the block associated to the bilinear form $a_2(\cdot, \cdot)$. The results are collected in the last row of Figure 5, where a much more pronounced swelling is observed far from the slip-displacement boundaries, whereas on the nonporous region, the material is swelling only due to the elastic compliance behavior.

Example 4: One-dimensional consolidation benchmark. In our last test we focus on the consolidation behavior of a thin porous column of height H and cross area W . The top and bottom surfaces of the column are endowed with pervious (zero pore pressure $p = 0$, constant mechanical load in the vertical direction $\sigma \mathbf{n} = -\sigma_0 \mathbf{e}_3$, and free to drain) and impervious (zero pressure flux $\kappa \nabla p \cdot \mathbf{n} = 0$ and zero displacement $\mathbf{u} = \mathbf{0}$) filtration conditions, respectively. On the lateral walls we enforce zero horizontal displacements (in both x_1 and x_2 directions). Therefore, Γ_p is the top side of the column, whereas $\Gamma_u = \partial\Omega \setminus \Gamma_p$. Moreover, we now consider the general time-dependent system (2.1)–(2.3), and our goal is to compare the obtained numerical approximations against the following exact solutions to the adimensional pseudo-one-

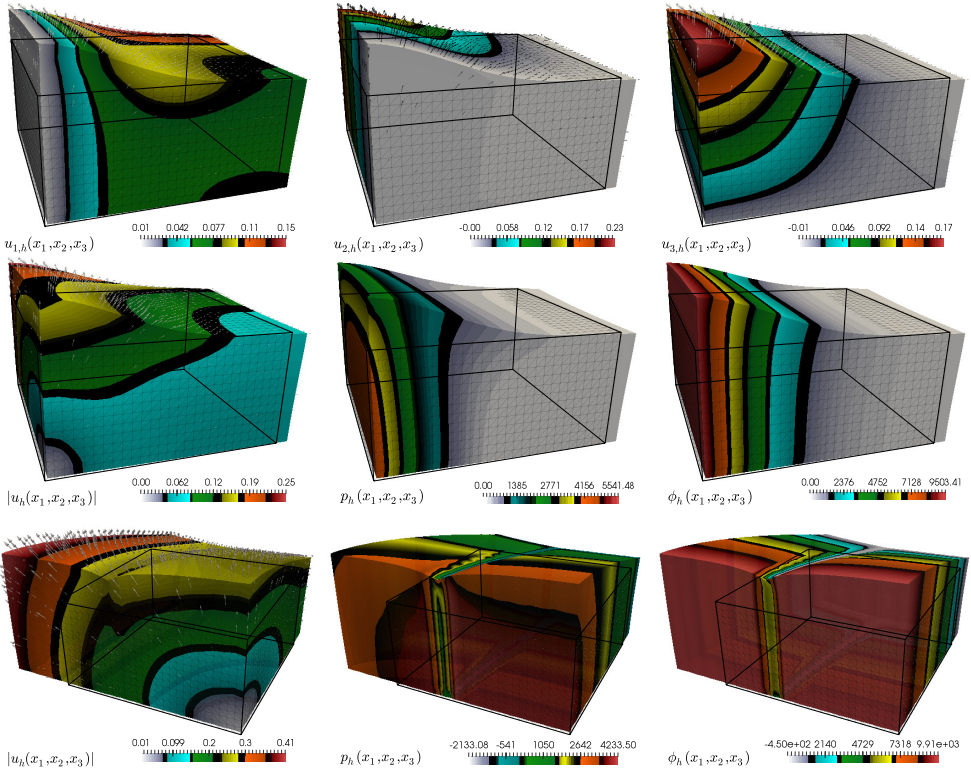


FIG. 5. Example 3: Swelling of a sponge using a stabilized method. This figure contains displacement components and magnitude, pressure distribution, and volumetric stress (top and middle row). The last row shows approximate solutions when a strip of zero permeability is present in the domain. All fields are represented on the deformed configuration, and the skeleton tetrahedral undeformed mesh is also depicted.

dimensional (1D) version of this problem (see, e.g., [32, 25, 29]):

$$u^* = 1 - x^* - \sum_{k=0}^{\infty} \frac{2}{M^2} \cos(Mx^*) \exp(-M^2 t^*), \quad p^* = \sum_{k=0}^{\infty} \frac{2}{M} \sin(Mx^*) \exp(-M^2 t^*),$$

where the superscript $*$ denotes adimensional quantities and variables as follows: $x^* = x_3/H$, $t^* = (\lambda + 2\mu)\kappa t H^2$, $M = \frac{1}{2}\pi(2k + 1)$, $u^* = u_3(\lambda + 2\mu)/\sigma_0 H$, $p^* = p/\sigma_0$.

As it stands, our analysis clearly does not cover the original time-dependent system, and our goal is only to illustrate the performance of the proposed schemes applied to (2.1)–(2.3). A semidiscretization of this problem using a backward Euler method with a fixed time-step Δt yields

$$(4.2) \quad \begin{aligned} a_1(\mathbf{u}_h^{n+1}, \mathbf{v}_h) + b_1(\mathbf{v}_h, \phi_h^{n+1}) &= F^{n+1}(\mathbf{v}_h) \quad \forall \mathbf{v}_h \in \mathbf{H}_h, \\ \tilde{a}_2(p_h^{n+1}, q_h) - b_2(q_h, \phi_h^{n+1}) &= \Delta t G^{n+1}(q_h) + \left(\frac{c_0}{\alpha} + \frac{1}{\lambda} \right) \int_{\Omega} p_h^n q_h - b_2(q_h, \phi_h^n) \quad \forall q_h \in Q_h, \\ b_1(\mathbf{u}_h^{n+1}, \psi_h) + b_2(p_h^{n+1}, \psi_h) - c(\phi_h^{n+1}, \psi_h) &= 0 \quad \forall \psi_h \in Z_h, \end{aligned}$$

with $\tilde{a}_2(p, q) := \left(\frac{c_0}{\alpha} + \frac{1}{\lambda} \right) \int_{\Omega} pq + \frac{\Delta t}{\alpha\eta} \int_{\Omega} \kappa \nabla p \cdot \nabla q$, which implies that at each time-step

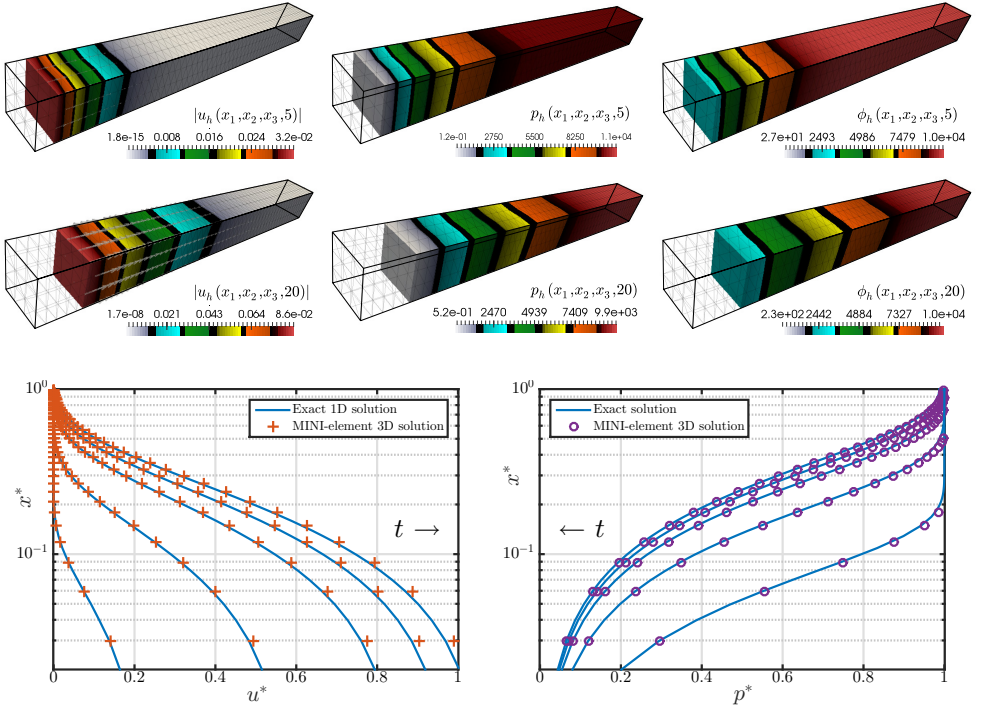


FIG. 6. Example 4: Consolidation benchmark using the MINI-element + Lagrange approximation together with a backward Euler time stepping. The first two rows show snapshots of the numerical solutions at $t = 5\text{ [s]}$ (top) and $t = 20\text{ [s]}$. The bottom row displays mid-line profiles of the computed versus exact nondimensional vertical displacement and pressure at five time instants $t^* = 0.2, 0.4, \dots, 1$.

we need to solve a system of the form (3.1)–(3.3). Notice that the coefficients in the left-hand side of the system are constant and so only the RHS needs to be reassembled at each time iteration. We choose the MINI-element + Lagrange approximation of displacement, volumetric stress and pressure, and the thin column with $H = 1\text{[m]}$, $W = 0.1\text{[m}^2]$ is discretized into a structured tetrahedral mesh containing 3312 elements. Model and numerical parameters assume the values $\sigma_0 = 1\text{e}4\text{ [Pa]}$, $E = 3\text{e}4\text{ [N/m}^2]$, $\nu = 0.2$, $\kappa = 1\text{e}-10\text{ [m}^2]$, $\eta = 1\text{e}-3\text{ [Pa s]}$, $c_0 = 0$, $\alpha = 1$, $\rho = 1$, $T = 10\text{ [s]}$, $\Delta t = 0.1\text{ [s]}$, and the initial data for displacement and pressure are set according to the idealized 1D solutions with the Fourier series truncated at $k = 350$. Figure 6 presents snapshots of the numerical solutions at early and advanced times, along with profiles of the computed approximations and exact adimensional solutions at the centerline (x_3 -axis) of the column, showing good accuracy throughout the time horizon.

We conclude this section stressing that the case of zero specific storage and zero Biot–Willis coefficient $c_0 = \alpha = 0$ is not covered in our present analysis, since the continuity and coercivity bounds for the pressure symmetric bilinear form $a_2(\cdot, \cdot)$ would blow up. Actually, the case $\alpha = 0$ is of less importance since it implies that the compression term, which in particular encodes the coupling of flow and deformations, vanishes. On the other hand, if the problem is rewritten as the Biot consolidation system after time discretization (as in (4.2)), then one realizes that the limit of $\Delta t \rightarrow 0$ only removes the stiffness part of the pressure in the modified bilinear form \tilde{a}_2 (see

also Example 3). Apart from having an ellipticity constant for a_2 independent of c_0 (which implies that all other important estimates such as Céa's lemma or stability are also independent of c_0), another possible way of treating the case $c_0 = 0$ consists of rewriting the problem as the three-field formulation recently analyzed in [23].

Natural extensions of this work include the development of conservative schemes based on finite volume elements and discontinuous Galerkin methods, and we also envisage the study of model generalizations to nonlinear (pressure dependent) permeability and finite deformations.

REFERENCES

- [1] G. AGUILAR, F. GASPAR, F. LISBONA, AND C. RODRIGO, *Numerical stabilization of Biot's consolidation model by a perturbation on the flow equation*, Internat. J. Numer. Methods Engrg., 75 (2008), pp. 1282–1300.
- [2] I. BABUŠKA AND A. AZIZ, *Survey lectures on the mathematical foundations of the finite element method*, in the Mathematical Foundations of the Finite Element Method with Applications to PDEs, Academic Press, New York, 1972, pp. 1–359.
- [3] S. BADIA, A. QUAINI, AND A. QUARTERONI, *Coupling Biot and Navier-Stokes equations for modelling fluid-poroelastic media interaction*, J. Comput. Phys., 228 (2009), pp. 7986–8014.
- [4] D. BAROLI, A. QUARTERONI, AND R. RUIZ-BAIER, *Convergence of a stabilized discontinuous Galerkin method for incompressible nonlinear elasticity*, Adv. Comput. Math., 39 (2013), pp. 425–443.
- [5] T. BARTH, P. BOCHEV, M. GUNZBURGER, AND J. SHADID, *A taxonomy of consistently stabilized finite element methods for the Stokes problem*, SIAM J. Sci. Comput., 25 (2004), pp. 1585–1607, doi:10.1137/S1064827502407718.
- [6] L. BERGER, R. BORDAS, D. KAY, AND S. TAVENER, *Stabilized lowest-order finite element approximation for linear three-field poroelasticity*, SIAM J. Sci. Comput., 37 (2015), pp. A2222–A2245, doi:10.1137/15M1009822.
- [7] M. A. BIOT, *Theory of elasticity and consolidation for a porous anisotropic solid*, J. Appl. Phys., 26 (1955), pp. 182–185.
- [8] D. BOFFI, *Stability of higher order triangular Hood-Taylor methods for stationary Stokes equations*, Math. Models Methods Appl. Sci., 2 (1994), pp. 223–235, doi:10.1142/S0218202594000133.
- [9] D. BOFFI, *Three-dimensional finite element methods for the Stokes problem*, SIAM J. Numer. Anal., 34 (1997), pp. 664–670, doi:10.1137/S0036142994270193.
- [10] Y. CHEN, Y. LUO, AND M. FENG, *Analysis of a discontinuous Galerkin method for the Biot's consolidation problem*, Appl. Math. Comput., 219 (2013), pp. 9043–9056.
- [11] C. DOMÍNGUEZ, G.N. GATICA, S. MEDDAHI, AND R. OYARZÚA, *A priori error analysis of a fully-mixed finite element method for a two-dimensional fluid-solid interaction problem*, ESAIM Math. Model. Numer. Anal., 47 (2013), pp. 471–506.
- [12] V. DOMÍNGUES AND F. J. SAYAS, *A BEM-FEM overlapping algorithm for the Stokes equation*, Appl. Math. Comput., 182 (2006), pp. 691–710.
- [13] A. ERN AND J.-L. GUERMOND, *Theory and Practice of Finite Elements*, Appl. Math. Sci. 159, Springer-Verlag, New York, 2004.
- [14] L. FRANCA, T. J. R. HUGHES, AND R. STENBERG, *Stabilized Finite Element Methods for the Stokes Problem*, Incompressible Computational Fluid Dynamics, M. Gunzburger and R.A. Nicolaides, eds., Cambridge University Press, Cambridge, UK, 1993, pp. 87–107.
- [15] F. J. GASPAR, F. J. LISBONA, AND C. W. OOSTERLEE, *A stabilized difference scheme for deformable porous media and its numerical resolution by multigrid methods*, Comput. Vis. Sci., 11 (2008), pp. 67–76.
- [16] G. N. GATICA, *A Simple Introduction to the Mixed Finite Element Method. Theory and Applications*, Springer Briefs in Mathematics, Springer, Cham, 2014.
- [17] G. N. GATICA, R. OYARZÚA, AND F. J. SAYAS, *Convergence of a family of Galerkin discretizations for the Stokes-Darcy coupled problem*, Numer. Methods Partial Differential Equations, 27 (2011), pp. 721–748.
- [18] G. N. GATICA, A. MÁRQUEZ, AND S. MEDDAHI, *Analysis of the coupling of primal and dual-mixed finite element methods for a two-dimensional fluid-solid interaction problem*, SIAM J. Numer. Anal., 45 (2007), pp. 2072–2097, doi:10.1137/060660370.

- [19] G. N. GATICA, R. OYARZÚA, AND F.J. SAYAS, *Analysis of fully-mixed finite element methods for the Stokes-Darcy coupled problem*, Math. Comp., 80 (2011), pp. 1911–1948.
- [20] V. GIRAUT AND P.-A. RAVIART, *Finite Element Approximation of the Navier-Stokes Equations*, Lecture Notes in Math. 749, Springer-Verlag, Berlin, New York, 1979.
- [21] P. GRISVARD, *Elliptic Problems in Nonsmooth Domains*, Classics Appl. Math. 69, SIAM, Philadelphia, 2011.
- [22] J. KORSAWE AND G. STARKE, *A least-squares mixed finite element method for Biot's consolidation problem in porous media*, SIAM J. Numer. Anal., 43 (2005), pp. 318–339, doi:10.1137/S0036142903432929.
- [23] J. J. LEE, *Guaranteed Locking-Free Finite Element Methods for Biot's Consolidation Model in Poroelasticity*, <http://arxiv.org/abs/1403.7038>, 2015.
- [24] R. LIU, M. F. WHEELER, C. N. DAWSON, AND R. H. DEAN, *On a coupled discontinuous/continuous Galerkin framework and an adaptive penalty scheme for poroelasticity problems*, Comput. Methods Appl. Mech. Engrg., 198 (2009), pp. 3499–3510, doi: 10.1016/j.cma.2009.07.005.
- [25] M. A. MURAD AND A. F. D. LOULA, *On stability and convergence of finite element approximations of Biot's consolidation problem*, Internat. J. Numer. Methods Engrg., 37 (1994), pp. 645–667.
- [26] M. A. MURAD, V. THOMÉE, AND A. F. D. LOULA, *Asymptotic behavior of semidiscrete finite-element approximations of Biot's consolidation problem*, SIAM J. Numer. Anal., 33 (1996), pp. 1065–1083, doi:10.1137/0733052.
- [27] P. J. PHILLIPS, *Finite Element Methods in Linear Poroelasticity: Theoretical and Computational Results*, Ph.D. thesis, The University of Texas at Austin, Austin, TX, 2005.
- [28] P. J. PHILLIPS AND M. F. WHEELER, *A coupling of mixed and continuous Galerkin finite element methods for poroelasticity I: The continuous in time case*, Comput. Geosci., 11 (2007), pp. 131–144.
- [29] R. RUIZ-BAIER AND I. LUNATI, *Mixed finite element – discontinuous finite volume element discretization of a general class of multicontinuum models*, J. Comput. Phys., 322 (2016), pp. 666–688, doi:10.1016/2016.06.054.
- [30] R. SHOWALTER, *Diffusion in poro-elastic media*, J. Math. Anal. Appl., 251 (2000), pp. 310–340.
- [31] K. STREHLOW, J. H. GOTTMANN, AND A. C. RUST, *Poroelastic responses of confined aquifers to subsurface strain and their use for volcano monitoring*, Solid Earth, 6 (2015), pp. 1207–1229.
- [32] K. TERZAGHI, *Theoretical Soil Mechanics*, Wiley, New York, 1943.
- [33] A. TRUTY, *A Galerkin/least-squares finite element formulation for consolidation*, Internat. J. Numer. Methods Engrg., 52 (2001), pp. 763–786.
- [34] R. UZUOKA AND R. I. BORJA, *Dynamics of unsaturated poroelastic solids at finite strain*, Int. J. Numer. Anal. Meth. Geomech., 36 (2012), pp. 1535–1573, doi:10.1002/nag.1061.
- [35] J. WAN, *Stabilized Finite Element Method for Coupled Geomechanics and Multiphase Flow*, Ph.D. thesis, Stanford University, Stanford, CA, 2002.
- [36] M. F. WHEELER, G. XUE, AND I. YOTOV, *Coupling multipoint flux mixed finite element methods with continuous Galerkin methods for poroelasticity*, Comput. Geosci., 18 (2014), pp. 57–75.
- [37] J. A. WHITE AND R. I. BORJA, *Stabilized low-order finite elements for coupled solid-deformation/fluid-diffusion and their application to fault zone transients*, Comput. Methods Appl. Mech. Engrg., 197 (2008), pp. 4353–4366.
- [38] S.-Y. YI, *Convergence analysis of a new mixed finite element method for Biot's consolidation model*, Numer. Methods Partial Differential Equations, 30 (2014), pp. 1189–1210.